2021-12-01

# Testing models of Laramide orogenic initiation by investigation of Late Cretace...





| Version | Published version |
| --- | --- |
| Citation (published version): | R.C. Economos, A.P. Barth, J.L. Wooden, S.R. Paterson, B. Friesenhahn, B.A. Wiegand, J.L. Anderson, J.L. Roell, E.F. Palmer, A.J. Ianno, K.A. Howard. 2021. "Testing models of Laramide orogenic initiation by investigation of Late Cretaceous magmatic-tectonic evolution of the central Mojave sector of the California arc." Geosphere, Volume 17, Issue 6, pp. 2042 - 2061. https://doi.org/10.1130/ges02225.1 |

https://hdl.handle.net/2144/44853

*Boston University*

Research Paper

GEOSPHERE

GEOSPHERE, v. 17, no. 6

https://doi.org/10.1130/GES02225.1

11 figures; 1 set of supplemental files

CORRESPONDENCE: reconomos@smu.edu

CITATION: Economos, R.C., Barth, A.P., Wooden, J.L., Paterson, S.R., Friesenhahn, B., Wiegand, B.A., Anderson, J.L., Roell, J.L., Palmer, E.F., Ianno, A.J., and Howard, K.A., 2021, Testing models of Laramide orogenic initiation by investigation of Late Cretaceous magmatic-tectonic evolution of the central Mojave sector of the California arc: Geosphere, v. 17, no. 6, p. 2042–2061, https://doi.org/10.1130/GES02225.1.

Science Editor: Shanaka de Silva
Associate Editor: G. Lang Farmer

Received 20 December 2019
Revision received 19 May 2021
Accepted 20 July 2021

Published online 5 November 2021



# Testing models of Laramide orogenic initiation by investigation of Late Cretaceous magmatic-tectonic evolution of the central Mojave sector of the California arc

**Rita C. Economos[1], Andrew P. Barth[2], Joseph L. Wooden[3], Scott R. Paterson[4], Brody Friesenhahn[1], Bettina A. Wiegand[5], J. Lawford Anderson[6], Jennifer L. Roell[2], Emerson F. Palmer[2], Adam J. Ianno[7], and Keith A. Howard[8]**

[1]Roy M. Huffington Department of Earth Sciences, Southern Methodist University, P.O. Box 750395, Dallas, Texas 75275-0395, USA
[2]Department of Earth Sciences, Indiana University/Purdue University Indianapolis, 723 West Michigan Street, Indianapolis, Indiana 46202, USA
[3]U.S. Geological Survey (Retired), Marietta, Georgia 30064, USA
[4]Department of Earth Sciences, University of Southern California, 3651 Trousdale Parkway, Los Angeles, California 90089, USA
[5]Applied Geoscience, University of Göttingen, Goldschmidtstrasse 3, Göttingen 37077, Germany
[6]Department of Earth and Environment, Boston University, 675 Commonwealth Avenue, Boston, Massachusetts 02215, USA
[7]Geology Department, Juniata College, 1700 Moore Street, Huntingdon, Pennsylvania 16652, USA
[8]U.S. Geological Survey, 345 Middlefield Road, Menlo Park, California 94025, USA

## ABSTRACT

**The Mojave Desert region is in a critical position for assessing models of Laramide orogenesis, which is hypothesized to have initiated as one or more seamounts subducted beneath the Cretaceous continental margin. Geochronological and geochemical characteristics of Late Cretaceous magmatic products provide the opportunity to test the validity of Laramide orogenic models. Laramide-aged plutons are exposed along a transect across the Cordilleran Mesozoic magmatic system from Joshua Tree National Park in the Eastern Transverse Ranges eastward into the central Mojave Desert. A transect at latitude ~33.5°N to 34.5°N includes: (1) the large upper-crustal Late Cretaceous Cadiz Valley batholith, (2) a thick section of Proterozoic to Jurassic host rocks, (3) Late Cretaceous stock to pluton-sized bodies at mesozonal depths, and (4) a Jurassic to Late Cretaceous midcrustal sheeted complex emplaced at ~20 km depth that transitions into a migmatite complex truncated along the San Andreas fault. This magmatic section is structurally correlative with the Big Bear Lake intrusive suite in the San Bernardino Mountains and similar sheeted rocks recovered in the Cajon Pass Deep Scientific Drillhole.**

**Zircon U-Pb geochronology of 12 samples via secondary ionization mass spectrometry (SIMS) (six from the Cadiz Valley batholith and six from the Cajon Pass Deep Scientific Drillhole) indicates that all Cretaceous igneous units investigated were intruded between 83 and 74 Ma, and Cajon Pass samples include a Jurassic age component. A compilation of new and published SIMS geochronological data demonstrates that voluminous magmatism in the Eastern Transverse Ranges and central Mojave Desert was continuous throughout the period suggested for the intersection and flat-slab subduction of the Shatsky Rise conjugate deep into the interior of western North America.**

**Whole-rock major-element, trace-element, and isotope geochemistry data from samples from a suite of 106 igneous rocks represent the breadth of Late Cretaceous units in the transect. Geochemistry indicates an origin in a subduction environment and intrusion into a crust thick enough to generate residual garnet. The lack of significant deflections of compositional characteristics and isotopic ratios in igneous products through space and time argues against a delamination event prior to 74 Ma.**

**We argue that Late Cretaceous plutonism from the Eastern Transverse Ranges to the central Mojave Desert represents subduction zone arc magmatism that persisted until ca. 74 Ma. This interpretation is inconsistent with the proposed timing of the docking of the Shatsky Rise conjugate with the margin of western North America, particularly models in which the leading edge of the Shatsky Rise was beneath Wyoming at 74 Ma. Alternatively, the timing of cessation of plutonism precedes the timing of the passage of the Hess Rise conjugate beneath western North America at ca. 70–65 Ma. The presence, geochemical composition, and age of arc products in the Eastern Transverse Ranges and central Mojave Desert region must be accounted for in any tectonic model of the transition from Sevier to Laramide orogenesis.**

R.C. Economos https://orcid.org/0000-0002-8484-7190

## INTRODUCTION

The transition from Sevier to Laramide orogenesis in the western United States was marked by major changes in tectonic style, faulting, and paleoelevation (Dickinson et al., 1978). A common feature of models for the tectonic evolution of this period is the migration of the locus of magmatism away from the continental margin (Coney and Reynolds, 1977; Copeland et al., 2017; Chapman et al., 2018), in some cases calling for near-horizontal (e.g., "flat") slab geometry due to the docking of the conjugates of the Shatsky and Hess

seamounts, currently located in the Pacific Ocean (Barth and Schneiderman, 1996; Saleeby, 2003; Liu et al., 2010; Heller and Liu, 2016). Although the major Laramide tectonic footprint is east of the Sierra Nevada batholith in Wyoming, Nevada, and Colorado (e.g., Bird, 1998), flat slab subduction cannot have occurred beneath the Sierra Nevada batholith due to the persistence of a deep arc keel until the Miocene (Ducea and Saleeby, 1998).

Models of the subduction of the Shatsky Rise conjugate hypothesize its passage through a relatively narrow zone of the Transverse Ranges and the Mojave Desert in southern California beginning at ca. 88 Ma. This hypothesis posits that the near-horizontal subduction of the Shatsky Rise conjugate propagated beneath the continental interior as far northeastward as Wyoming by ca. 74 Ma (Saleeby, 2003; Liu et al., 2010). Significant magmatism in the Mojave region is proposed to have ceased at ca. 85 Ma (Liu et al., 2010), as the eastward migration of the locus of magmatism and the subsequent cessation of magmatism are considered to have been primary responses to this event (Copeland et al., 2017).

However, post–85 Ma Cretaceous igneous units are widely recognized in the Eastern Transverse Ranges and central Mojave region (e.g., Powell, 1981; Calzia et al., 1986; Barth et al., 2004; Wells and Hoisch, 2008; Needy et al., 2009). Fitting these plutons into the hypothesis of a cessation of arc magmatism at ca. 85 Ma requires an asthenospheric contribution of heat and material to the magmatic system and lithospheric thinning due to delamination. Such a scenario was proposed for plutonism in the eastern Mojave Desert by Wells and Hoisch (2008), although for a later slab egress at ca. 75 Ma.

These tectonic hypotheses are thus testable by assessing the ages and geochemical characteristics of plutons in the Eastern Transverse Ranges and central Mojave region. The predictions for magmatism occurring after passage of a middle–Late Cretaceous flat slab in this region are: (1) abundant magmatism ceased ca. 85 Ma, (2) asthenospheric input provided the heat source for subsequent magmatism, and (3) plutons were generated in a crust that was thinned by delamination. If these predictions are correct, we would expect asthenospheric input to the magmatic system to be indicated by the presence of isotopically primitive igneous products, and changes in the crustal thickness of the magmatic column should have yielded shifts in characteristic trace-element ratios of magmatic products (e.g., Profeta et al., 2015; Lieu and Stern, 2019).

Alternatively, if Mojave Desert plutons were generated in an arc environment, similar to the Sierra Nevada batholith and the Peninsular Ranges batholith, this would constrain the timing of possible flat slab subduction beneath this region as postdating plutonism, leaving no viable route for the flat slab to move into the interior of western North America at ca. 88–74 Ma.

The purpose of this study was to highlight the abundance, extent, timing, and character of Late Cretaceous plutonic rocks in the Eastern Transverse Ranges and central Mojave Desert region. These plutonic rocks represent a fundamental and chronologically constrained record of a region that is critical in understanding the evolution of the plate margin at the onset of the Laramide orogeny. The Late Cretaceous Cadiz Valley batholith (Fig. 1; Howard, 2002; Barth et al., 2004) was uniquely situated in time and space to have been affected by possible passage of the Shatsky Rise conjugate. The interpretation of the origin of this batholith is critical because it provides the evidence of voluminous, focused input of magmas into the upper crust.

The study area of the Transverse Ranges and Mojave Desert segment of the continental margin has been significantly disrupted and, in some cases (e.g., the San Gabriel Mountains and the Tehachapi Range), deeply exhumed (Barth

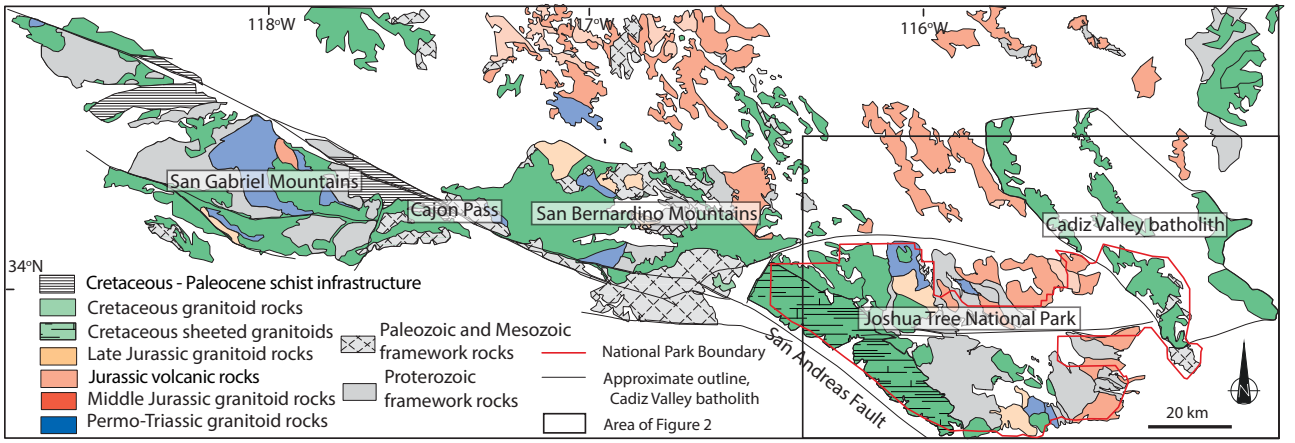


**Figure 1. Geologic map of the Transverse Ranges, adapted from Powell (1993), Howard (2002), Needy et al. (2009), and Powell et al. (2015), depicting regional extent of Cretaceous magmatism and the main components of the Transverse Ranges tilted arc crustal section. The sheeted complex, shown as hachured areas, extends from southern Joshua Tree National Park to Cajon Pass.**

and May, 1992; Pickett and Saleeby, 1993; Nadin and Saleeby, 2008). Also, the underplating of the Pelona-Orocopia-Rand family of schists and associated rocks attests to significant subduction-erosion in the region (Haxel and Dillon, 1978; Jacobson et al., 2000; Grove et al., 2003). Subsequent faulting dissected the Mojave Desert segment of the Mesozoic margin to a greater extent than the Sierra Nevada batholith to the north and the Peninsular Ranges batholith to the south, resulting in variable depths of crustal exposure in the Mojave Desert. This exposure allows for a more complete investigation of the crustal evolution of the Mojave Desert segment of the Cretaceous Cordilleran belt.

## GEOLOGIC SETTING

The Transverse Ranges include the San Gabriel Mountains, San Bernardino Mountains, and the mountain ranges that occur in Joshua Tree National Park (Fig. 1). The San Andreas fault divides the Transverse Ranges, separating the San Gabriel Mountains from the San Bernardino Mountains. In order to avoid the necessity of palinspastic reconstructions, we dealt only with regions on the eastern (North American) side of the San Andreas fault, and thus we define our study area as the Eastern Transverse Ranges, including the San Bernardino Mountains and Joshua Tree National Park. The study area extends east into the central Mojave Desert to encompass the Cadiz Valley batholith, which is truncated at its eastern margin by the major "breakaway" faults that mark the boundary of Basin and Range extension, sensu stricto, of the Colorado River extensional corridor (Wells et al., 2005).

### Host Rocks: Proterozoic Basement and Early–Middle Mesozoic Intrusive Units

In contrast to the Sierra Nevada batholith, where pre-Mesozoic units are preserved only in small and strongly deformed metasedimentary pendants, large blocks of Proterozoic basement are preserved throughout the Eastern Transverse Ranges area. Basement rocks record a complex Proterozoic history as is typical of the Mojave crustal province. The oldest rocks presently exposed in the Mojave are metaigneous rocks and continental sediments dating from 1790 to 1730 Ma, which predate a period of major tectonism, chronologically correlative with the Ivanpah orogeny of Wooden and Miller (1990). From 1690 to 1640 Ma, igneous units were intruded contemporaneously with continued regional metamorphism, migmatization, isoclinal folding, and west-vergent shearing (Barth et al., 2009; Strickland et al., 2013). This Paleoproterozoic crust was further intruded by a range of Mesoproterozoic plutons, the most voluminous in the Mojave Desert being granitic to syenitic plutons emplaced from 1430 to 1400 Ma throughout North America (Anderson and Bender, 1989; Anderson and Morrison, 1992).

The heterogeneity of exposed Proterozoic rocks suggests potentially diverse crustal sources for Mesozoic magmas (e.g., Barth et al., 1992). Early recognition of crustal source heterogeneity in the Mojave Province stemmed from studies of bulk zircon isotopic systematics of Late Cretaceous intrusive rocks that yielded both Paleoproterozoic and Mesoproterozoic intercept ages correlated to major Proterozoic magmatic events (Wright et al., 1987; Miller et al., 1992).

Isotopic compositions of plutonic rocks also reflect the presence of Proterozoic basement in the region. Data from intrusive rocks of the Transverse Ranges magmatic rocks are consistently more enriched in radiogenic isotopes than rocks of similar major-element compositions in the Sierra Nevada batholith (DePaolo, 1981; Kistler and Ross, 1990; Chen and Tilton, 1991; Paterson et al., 2017). The most geochemically primitive rocks in the region yield $^{87}Sr/^{86}Sr_{(t)}$ values from 0.707 to 0.709 and $\varepsilon Nd_{(t)}$ values lower than –10, despite their mafic composition; evolved rocks yield $^{87}Sr/^{86}Sr_{(t)}$ values up to ~0.714 and $\varepsilon Nd_{(t)}$ values as low as –17 (Barth et al., 1992, 1995; Mayo et al., 1998; Wiegand et al., 2007; this study).

Three Mesozoic magmatic pulses that are characteristic of the Cordilleran arc are preserved in the field area. Triassic plutons are alkali-calcic quartz monzodiorites and monzonites present in relatively small volumes (Fig. 2; Barth et al., 1997). Significant Jurassic plutonism occurred in the eastern Joshua Tree National Park, with intrusion ages ranging from ca. 165 to 161 Ma (Barth et al., 2008, 2017; Howard et al., 2013, and references therein). This includes a Jurassic batholith consisting of plutonic to hypabyssal quartz monzonites that is the host rock for the Cadiz Valley batholith along its western margin (Howard, 2002; Howard et al., 2013). Smaller, typically calc-alkaline, Jurassic plutons with ages of 152–150 Ma are located in the western and southwestern portions of Joshua Tree National Park and are interleaved with Cretaceous igneous sheets in the Little San Bernardino Mountains (Needy et al., 2009).

### Cretaceous Magmatic Crustal Section

Needy et al. (2009) argued that in Joshua Tree National Park, Cretaceous intrusive rocks are exposed from shallow crustal levels to ~20 km depth, broken only by moderate to minor faults that do not omit significant section, although at least one extensional fault in the Pinto Mountains juxtaposes structural levels (Howard et al., 2013). The regional structural style was interpreted as a monoclinal or homoclinal structure steepening toward the San Andreas fault. This region represents a crustal section through the Mesozoic crust presently tilted at ~8° about a NNW-trending axis. The range of thermobarometric mineral assemblages in Cretaceous igneous rocks indicates that differential uplift occurred across the Eastern Transverse Ranges and central Mojave Desert following the cessation of magmatism, exposing deeper portions of the crust in the south and west (Anderson, 1988; Barth, 1990; Barth and May, 1992; Needy et al., 2009; Ianno, 2015).

The Cadiz Valley batholith, an ~600 km$^2$ (exposed) batholith located in the central Mojave Desert, which spans the region from the Coxcomb and Sheep Hole Mountains to the Iron Mountains, is composed of the shallowest plutons in the field area (Calzia, 1982; Howard, 2002). The Cadiz Valley batholith intrudes

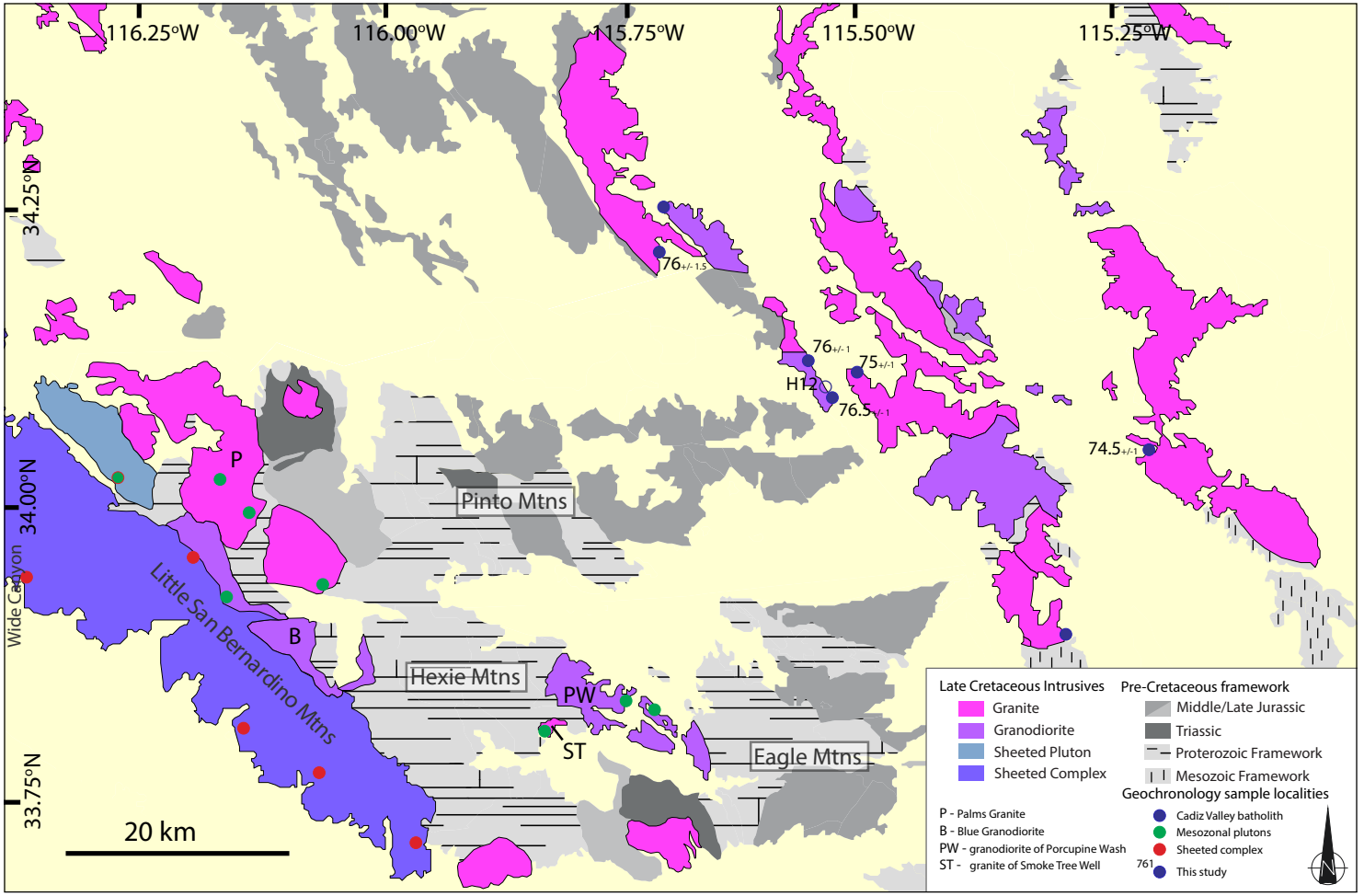


**Figure 2. Geologic map of Late Cretaceous intrusive rocks of the Cadiz Valley batholith and structurally lower intrusive units of the Eastern Transverse Ranges magmatic arc crustal section. See Figure 1 for location. Locations of geochronology samples (new and published) and significant units discussed in the text are noted. Mtns—Mountains.**

Jurassic plutons in the west and the Late Jurassic to mid–Late Cretaceous metasedimentary McCoy Mountains Formation in the south (Fig. 2; Barth et al., 2004). Compositions range from volumetrically dominant muscovite/biotite monzogranite to biotite-hornblende granodiorite in the southern Coxcomb Mountains (Calzia, 1982; Howard, 2002). Late Cretaceous zircon U-Pb ages ranging from 77 to ca. 70 Ma have been reported (Calzia et al., 1986; Barth et al., 2004; Wells and Hoisch, 2008; Chapman et al., 2018). An Al-in-hornblende barometry result from the southeastern part of the batholith indicated an emplacement depth of ~6 km (Anderson, 1988), a shallow structural position that is consistent with the crustal level inferred from eastward projection of the depth transect of Needy et al. (2009). The batholith is, however, partly disrupted by east-dipping Miocene normal faults (Howard, 2002).

West of the Cadiz Valley batholith, the next exposed Cretaceous plutons in the field area are in the west-central region of Joshua Tree National Park, in the eastern Hexie Mountains and western Pinto Mountains (Fig. 2), where various granite and granodioritic plutons intrude Proterozoic basement rocks.

We collectively refer to these plutons as "mesozonal" in reference to their 10–16 km emplacement depths (Needy et al., 2009; Ianno, 2015). Contacts between plutons and Proterozoic host rocks are typically steeply to moderately dipping and are variably discordant to the steeply dipping Proterozoic metamorphic foliations. This group of plutons includes the biotite-hornblende Blue granodiorite and the granodiorite of Porcupine Wash, the weakly metaluminous Palms Granite, and the weakly peraluminous granite of Smoke Tree Well (Fig. 2).

The deepest of the exposed magmatic rocks in the field area form a sheeted complex of tonalite to granodiorite and biotite ± muscovite ± garnet granites that concordantly intrude foliated Proterozoic gneisses (Fleck et al., 1997; Wooden et al., 2001; Barth et al., 2008; Ianno, 2015). Igneous intrusions consist of mainly meter- to decimeter-scale sheets with some larger, lenticular stock-sized bodies. Needy et al. (2009) summarized the field characteristics and geochronology of the sheeted complex, which indicate its construction during two stages, one in the Late Jurassic and one in the Late Cretaceous. Intrusive depths of ~15–19 km were reported for plutonic rocks from the Little San Bernardino Mountains and in the westernmost Joshua Tree National Park (Needy et al., 2009; Ianno, 2015).

This sheeted complex often appears along a mappable contact with lenticular-shaped plutons that intrude along the western margins of the mesozonal Palms Granite and Blue granodiorite (Ianno, 2015). Dips average ~40° to the east, and intrusive bodies are concordant with metamorphic wall rocks that are present throughout the complex. The dominant planar fabric in the complex is defined by metamorphic foliations, magmatic contacts between sheets, and alignment of high-aspect-ratio magmatic minerals (Ianno, 2015).

Finally, the deepest exposures in the Little San Bernardino Mountains are transected by the north-south–trending Wide Canyon. Here, sheeted rocks transition into a less structurally coherent migmatitic zone of both Proterozoic and Cretaceous age (Friesenhahn, 2018). Rocks of this style are truncated to the west by the San Andreas fault.

The characteristics of these Late Cretaceous intrusions are paralleled by those in the San Bernardino Mountains, which lie to the northwest of the tilted crustal section in Joshua Tree National Park. Mapping by Powell (1993) indicated that the San Bernardino mountain range is located structurally along strike of plutons in Joshua Tree National Park (Fig. 1). This range includes a Late Cretaceous upper-crustal batholith, the Big Bear Lake intrusive suite (Morton and Miller, 2003; Barth et al., 2016). The Big Bear Lake intrusive suite is similar to the Cadiz Valley batholith in size, composition, and age and was emplaced at slightly deeper crustal levels (Barth et al., 2016). Structurally beneath the Big Bear Lake intrusive suite, there is a unit similar to the sheeted complex in Joshua Tree National Park, which was sampled by the deep scientific drill core in Cajon Pass on the northwestern edge of the San Bernardino Mountains (Cajon Pass Deep Scientific Drillhole [Federal 2–26]; Wicklund et al., 1990; Pratson et al., 1992; Barth and Dorais, 2000). Below ~1.2 km depth, drillers recovered samples of a sheeted, heterogeneous plutonic unit that represents a crustal thickness of at least 2 km. The shallowly dipping, foliated intrusive bodies range in composition from tonalite and diorite through granodiorite to granite. An intrusive pressure of 6 ± 1 kbar was calculated from hornblende-plagioclase thermobarometry and is consistent with the presence of epidote in the magmatic assemblage of tonalitic samples (Barth and Dorais, 2000). Zircon U-Pb ages from these samples presented here will test the projection of the oblique tilted crustal section into the San Bernardino Mountains (e.g., Barth et al., 2016).

## METHODS

### Geochronology

We present new secondary ionization mass spectrometry (SIMS) zircon U-Pb ages for upper-crustal and sheeted midcrustal plutonic rocks (Figs. 3 and 4) and a compilation of all published SIMS U-Pb geochronology in zircon for Late Cretaceous igneous rocks from the study area (Fig. 5). The goal was to investigate the timing relationships between intrusions as a function of depth in the oblique exposure and between intrusions at similar paleodepths along strike across the Transverse Ranges. Analysis by SIMS allowed for sampling of magmatic zircon rims and avoidance of Proterozoic cores, which are ubiquitous in zircons from Cretaceous granitoid rocks of the entire Eastern Transverse Ranges and Mojave Desert region. Also included are new ages from samples recovered from the Cajon Pass Deep Scientific Drillhole. Samples from units 2 through 5 of Barth and Dorais (2000) were selected based on the quality of core recovery. Samples ~10 $cm^3$ in size were processed for zircon separation at Iowa State University and yielded sufficient zircon fractions for SIMS analysis. Cadiz Valley batholith geochronology samples were selected to represent the compositional diversity observed in the batholith (Howard, 2002). U-Pb data were collected using the U.S. Geological Survey (USGS)–Stanford sensitive high-resolution ion microprobe–reverse geometry (SHRIMP-RG) at Stanford University utilizing analytical and data reduction procedures described by Barth and Wooden (2006). Isotope ratios were calibrated against Braintree zircon standard R33, with an age of 419 Ma (Black et al., 2004). Zircon spot ages are reported at the 1σ level (Tables S1 and S2[1]), and interpreted crystallization ages of rocks are reported as the weighted mean age with errors at the 2σ level.

### Whole-Rock Geochemistry

The whole-rock elemental data (Table S3 [see footnote 1]) presented here include samples from the Cadiz Valley batholith, mesozonal plutons, and the sheeted complex. These were analyzed by X-ray fluorescence (XRF) and inductively coupled plasma–mass spectrometry (ICP-MS) at Michigan State University (MSU). Additional whole-rock samples from the southern Cadiz Valley batholith in the Coxcomb Mountains were analyzed by XRF at the University of Southern California (USC). Despite slight differences in preparation, we consider the data sets comparable because both display similar trace-element

Table S1. SHRIMP U-Pb zircon data for Cadiz Valley Batholith rocks

| | ppm | ppm | 238U/ | | 207Pb/ | | 206Pb*/238U | | 207Pb*/206Pb* | |
|---|---|---|---|---|---|---|---|---|---|---|
| | U | Th | 206Pb* | err | 206Pb | err | Age | err | Age | err |
| **Sheep Hole Pass Granite** | | | | | | | | | | |
| **09-758** | **3783719*** | **617682** | | | | | | | | |
| 758-3 | 129 | 78 | 88.88 | 2.0 | 0.0622 | 6.8 | 70.8 | 1.5 | | |
| 758-9 | 132 | 92 | 87.56 | 2.0 | 0.0551 | 7.0 | 72.5 | 1.5 | | |
| 758-10 | 279 | 166 | 87.51 | 1.3 | 0.0546 | 4.8 | 72.6 | 1.0 | | |
| 758-8 | 161 | 38 | 86.25 | 1.8 | 0.0607 | 6.0 | 73.1 | 1.3 | | |
| 758-14 | 118 | 201 | 86.93 | 1.9 | 0.0543 | 6.8 | 73.1 | 1.4 | | |
| 758-1 | 367 | 210 | 86.52 | 1.1 | 0.0505 | 4.3 | 73.8 | 0.9 | | |
| 758-4 | 151 | 40 | 85.38 | 1.8 | 0.0534 | 6.6 | 74.5 | 1.4 | | |
| 758-6 | 2694 | 1259 | 84.76 | 0.9 | 0.0483 | 1.6 | 75.5 | 0.6 | | |
| 758-5 | 1289 | 1603 | 83.74 | 0.6 | 0.0462 | 2.4 | 76.7 | 0.5 | | |
| 758-7 | 4413 | 326 | 83.06 | 0.3 | 0.0493 | 1.5 | 77.0 | 0.3 | | |
| 759-11 | 240 | 174 | 83.41 | 1.1 | 0.0495 | 4.2 | 100.7 | 1.2 | | |
| 759-12 | 1197 | 696 | 43.86 | 0.5 | 0.0555 | 1.5 | 140.0 | 0.7 | | |
| 759-15 | 191 | 267 | 42.71 | 1.1 | 0.0485 | 4.1 | 146.3 | 1.7 | | |
| 759-13 | 176 | 188 | 40.60 | 1.1 | 0.0548 | 3.7 | 154.4 | 1.7 | | |
| 759-2 | 551 | 445 | 37.67 | 0.7 | 0.0555 | 2.3 | 168.7 | 1.1 | | |
| **Granodiorite of Clark's Pass** | | | | | | | | | | |
| **09-760** | **3772416** | **633916** | | | | | | | | |
| 760-13 | 59 | 86 | 87.63 | 2.6 | 0.0667 | 8.5 | 71.4 | 1.9 | | |
| 760-8 | 171 | 166 | 85.90 | 1.9 | 0.0547 | 7.2 | 73.9 | 1.5 | | |
| 760-5 | 622 | 347 | 85.02 | 0.9 | 0.0503 | 3.3 | 75.1 | 0.7 | | |
| 760-10 | 395 | 236 | 84.33 | 1.1 | 0.0508 | 3.8 | 75.1 | 0.8 | | |
| 760-7 | 943 | 326 | 85.14 | 0.8 | 0.0478 | 3.0 | 75.3 | 0.6 | | |
| 760-9 | 551 | 243 | 84.01 | 0.9 | 0.0504 | 3.5 | 76.0 | 0.7 | | |
| 760-2 | 397 | 112 | 83.67 | 1.1 | 0.0493 | 5.0 | 76.4 | 0.9 | | |
| 760-3 | 2061 | 945 | 83.08 | 0.5 | 0.0483 | 1.8 | 77.1 | 0.4 | | |
| 760-1 | 317 | 295 | 81.75 | 1.4 | 0.0605 | 4.2 | 77.1 | 1.1 | | |
| 760-4 | 1260 | 489 | 82.68 | 0.6 | 0.0502 | 2.3 | 77.2 | 0.5 | | |
| 760-12 | 1212 | 132 | 58.64 | 0.5 | 0.0677 | 1.6 | 108.3 | 0.6 | | |
| 760-6 | 1246 | 1110 | 82.94 | 0.6 | 0.0514 | 2.3 | 76.9 | 0.5 | | |
| 760-14 | 171 | 60 | 6.03 | 0.6 | 0.0919 | 1.1 | 966.9 | 6.1 | 1472 | 47 |
| 760-11 | 163 | 106 | 3.52 | 0.7 | 0.1030 | 0.9 | 1658.5 | 10.4 | 1682 | 30 |
| **Clarks Pass Granodiorite** | | | | | | | | | | |
| **ND45** | **3774402** | **632266** | | | | | | | | |
| ND45-3 | 139 | 103 | 92.48 | 1.8 | 0.0491 | 6.7 | 69.2 | 1.2 | | |
| ND45-2 | 530 | 345 | 89.49 | 1.0 | 0.0497 | 3.4 | 71.4 | 0.8 | | |
| ND45-4 | 366 | 313 | 87.46 | 1.1 | 0.0499 | 4.0 | 73.1 | 0.8 | | |
| ND45-5 | 316 | 104 | 86.98 | 1.1 | 0.0492 | 4.3 | 73.5 | 0.9 | | |
| ND45-6 | 355 | 169 | 85.72 | 1.1 | 0.0485 | 4.8 | 74.7 | 0.8 | | |
| ND45-11 | 635 | 349 | 84.91 | 0.8 | 0.0510 | 3.0 | 75.2 | 0.6 | | |
| ND45-12 | 255 | 240 | 84.97 | 1.3 | 0.0499 | 4.6 | 75.2 | 1.0 | | |
| ND45-7 | 564 | 339 | 84.10 | 0.8 | 0.0472 | 3.2 | 76.2 | 0.6 | | |
| ND45-10 | 710 | 1569 | 83.52 | 0.8 | 0.0484 | 2.9 | 76.6 | 0.6 | | |
| ND45-1 | 575 | 309 | 83.37 | 0.9 | 0.0472 | 3.4 | 76.9 | 0.7 | | |
| ND45-8 | 402 | 181 | 82.69 | 1.0 | 0.0474 | 3.8 | 77.5 | 0.8 | | |
| ND45-9 | 339 | 617 | 82.27 | 1.1 | 0.0474 | 4.1 | 77.9 | 0.9 | | |

[1]Supplemental Material. Table S1: SHRIMP zircon U-Pb geochronology data for six samples from the Cadiz Valley batholith. Table S2: SHRIMP zircon U-Pb geochronology data for six samples from the Federal 2-26 Cajon Pass drill core. Table S3: Whole-rock major- and trace-element geochemistry of granitic rocks from Joshua Tree National Park and the Cadiz Valley batholith measured by X-ray fluorescence (XRF) and inductively coupled plasma–mass spectrometry (ICP-MS). Table S4: Rb/Sr and Sm/Nd isotope data from the Joshua Tree National Park and Cadiz Valley batholith. Table S5: Locations, data, and references used to generate histograms in Figure 5. Please visit https://doi.org/10.1130/GEOS.S.15121998 to access the supplemental material, and contact editing@geosociety.org with any questions.

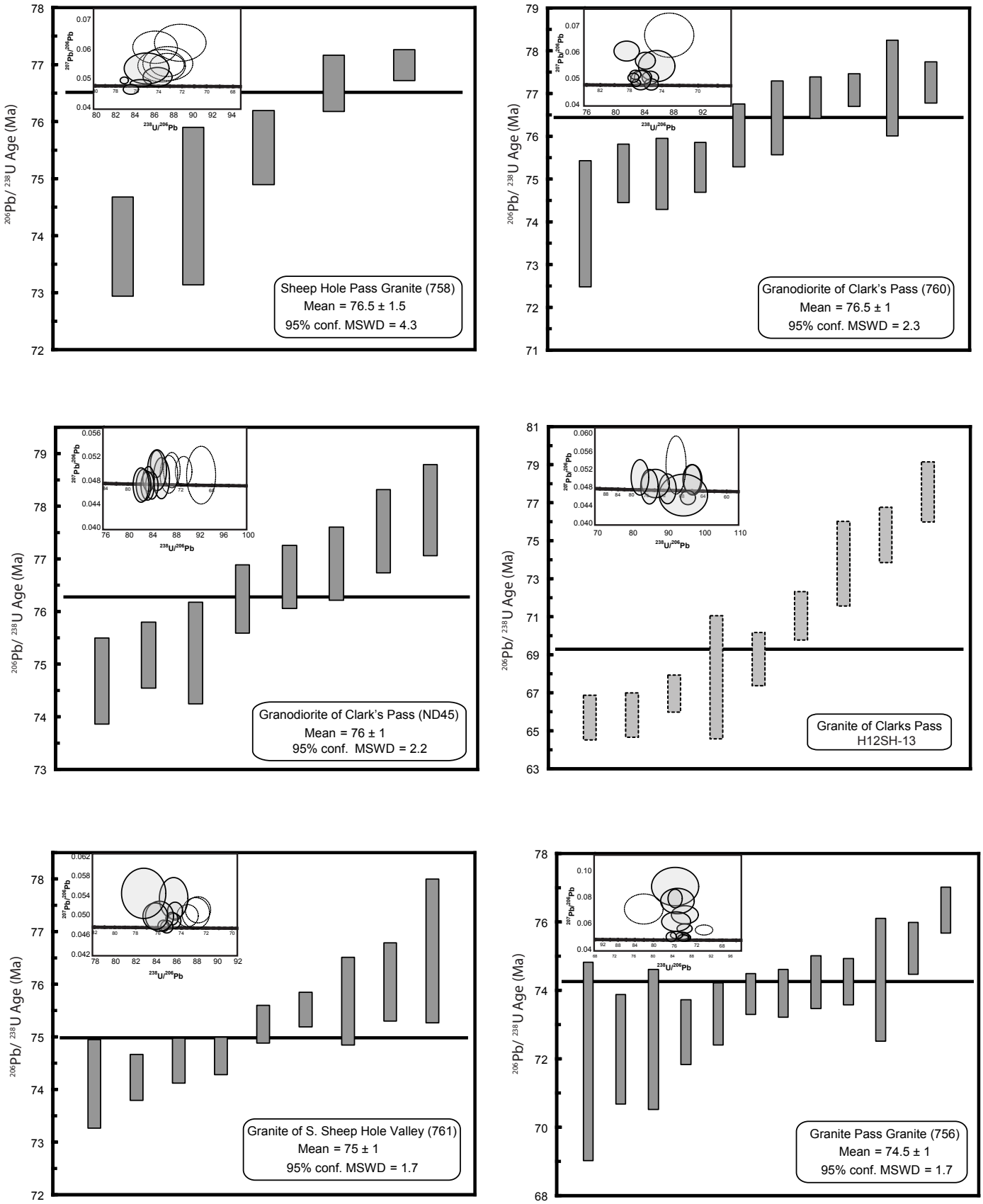


**Figure 3. Tera-Wasserburg concordia diagrams and weighted mean $^{206}Pb^*/^{238}U$ ages for zircons from six samples from the upper-crustal Cadiz Valley batholith. Ages are weighted means with errors cited at 2σ. All measured zircons are plotted on concordia diagram insets; zircon analyses plotted with unshaded symbols were excluded from calculation of crystallization ages (see text for discussion). MSWD—mean square of weighted deviates.**

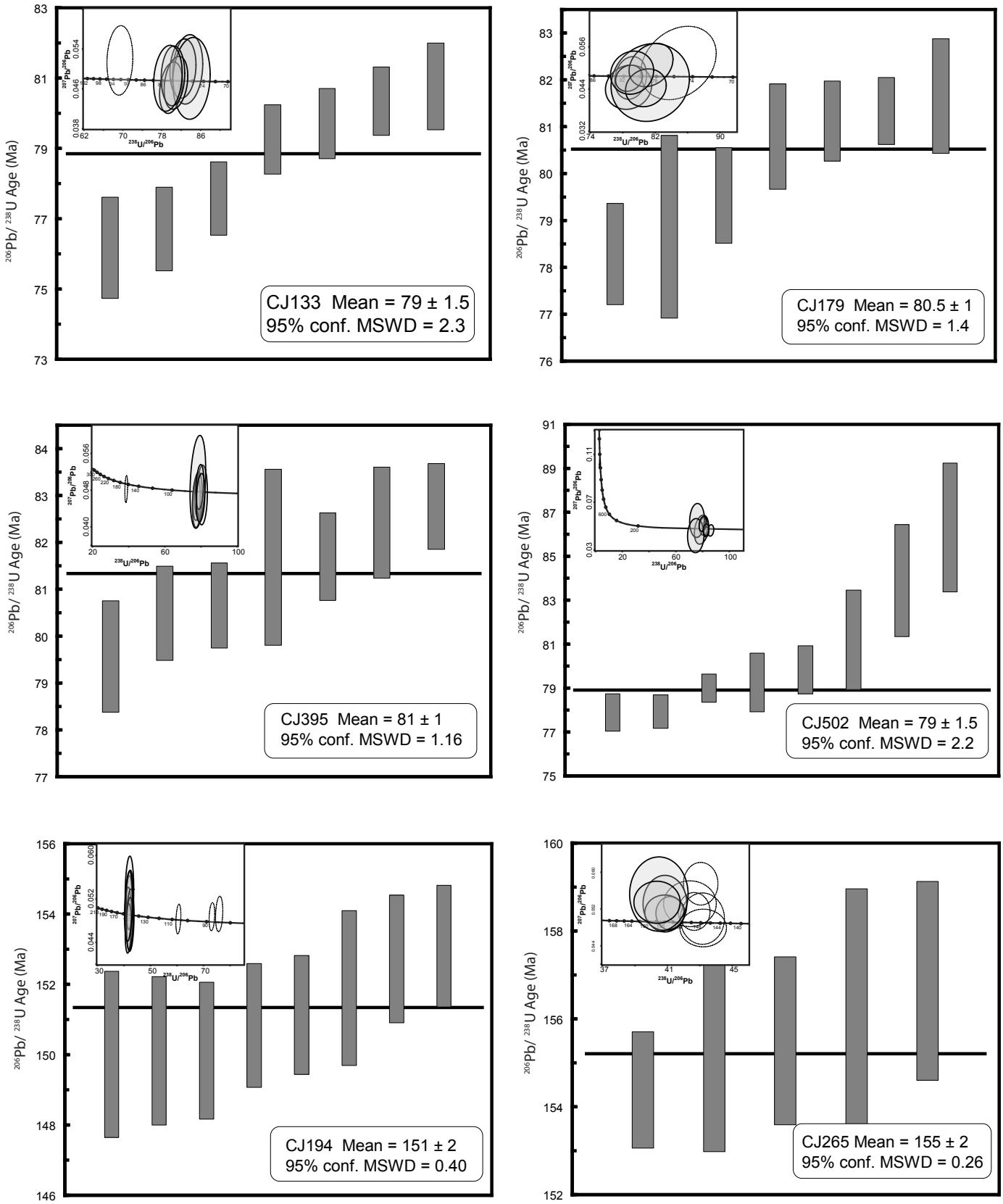


**Figure 4. Tera-Wasserburg concordia diagrams and weighted mean $^{206}Pb^*/^{238}U$ ages for zircons from six samples from the midcrustal rocks of the Cajon Pass drill hole. Ages are weighted means with errors cited at 2σ. All measured zircons are plotted on concordia diagram insets; zircon analyses plotted with unshaded symbols were excluded from calculation of crystallization ages (see text for discussion). MSWD—mean square of weighted deviates.**

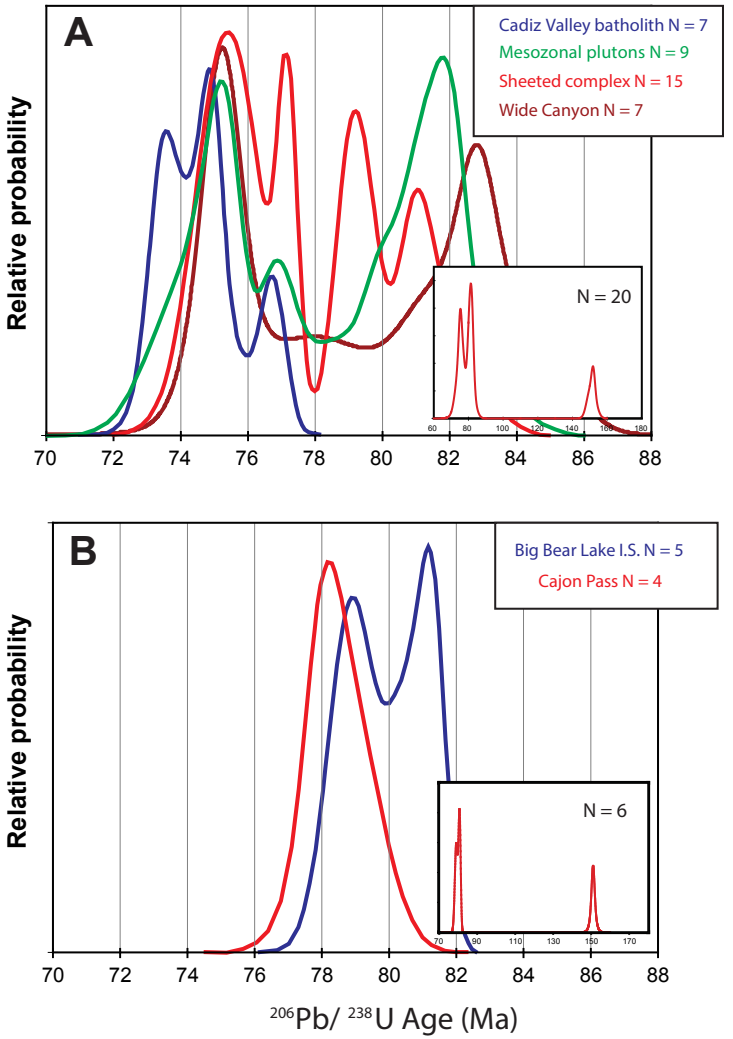


**Figure 5. Compilation of Cretaceous ages from secondary ionization mass spectrometry (SIMS) U-Pb in zircon geochronology for the Eastern Transverse Ranges magmatic arc crustal section (Barth et al., 2004, 2009; Needy et al., 2009; Friesenhahn, 2018; this study). See Figures 1 and 2 for sample locations. Hot colors indicate deeper paleodepths; cool colors indicate shallower paleodepths. (A) Comparison of ages of Cadiz Valley batholith to structurally lower, intermediate-depth plutons and rocks of the midcrustal sheeted complex and Wide Canyon in Joshua Tree National Park. (B) Comparison of ages from the arc crustal section in the San Bernardino Mountains, including the Big Bear Lake intrusive suite and structurally lower sheeted rocks from the Cajon Pass drill hole. Probability density functions were calculated using Isoplot. Insets show all geochronology from the sheeted complex (A) and the Cajon Pass drill core (B), including interspersed Jurassic sheets.**

compositional trends that are particular to magmatic rocks in this region. All samples were crushed in steel and tungsten carbide jaw crushers and were powdered using tungsten carbide ball mills. Samples were fused into lithium borate glasses for major-element oxide analysis, but trace-element measurements for USC samples were conducted on briquetted rock powders, while trace elements were analyzed directly on glass disks at MSU. Measurements at USC were conducted on a Rigaku XRF spectrometer, and MSU analyses were conducted on a Bruker S4 PIONEER XRF spectrometer. Errors on USC samples are between 1% and 5% analyzed quantity for major and trace elements. For MSU samples, major-element oxides have errors of <1%, Sr measurements have errors of <1%, and Y and Rb have errors of <5%.

Additional trace-element analyses were collected by solution ICP-MS at MSU. Reproducibility of unknowns was checked against rock standard JB-1a. Reproducibility on large ion lithophile elements (LILEs), Zr, La, V, and Cr was 2%–2.5%. Reproducibility for all other elements, including rare earth elements (REEs), was ≤5%.

Measurements of Sr and Nd isotope ratios were mainly conducted on a Finnigan MAT 261 thermal ionization mass spectrometer at the Stanford University Microanalytical Center (Table S4 [footnote 1]). The data set was augmented by analyses on two VG Sector 54 thermal ionization mass spectrometers at the University of North Carolina and the University of Arizona. Samples analyzed at the University of Arizona were spiked for Sm and Nd so that concentrations could be measured directly. Whole-rock concentrations of Rb and Sr in other samples were determined by XRF and used to calculate Rb/Sr; a value of 0.14 Sm/Nd was assumed for ratio calculations on samples analyzed at Stanford. All samples had Rb/Sr ratios ≤3, precluding large errors introduced by high-Rb samples. Isotope measurements were calibrated against NBS987 (Sr) and AMES (Nd) (Wiegand et al., 2007).

## RESULTS

### Geochronology of Upper-Crustal Batholithic Rocks

Six samples from the Cadiz Valley batholith yielded equant to prismatic grains that displayed fine oscillatory zoning in cathodoluminescence (CL) images. Some zones were dark in CL images, suggesting high U content. Discordant cores, interpreted as inherited zircons, were observed in most samples, necessitating the use of a focused beam (in situ) dating technique such as SIMS. Some Pb loss, identified by a spread of ages along the Tera-Wasserburg concordia, was observed in all samples (Fig. 3). We selected the most coherent population in each sample, excluding some grains with indications of Pb loss. This strategy yielded a mean square of weighted deviates (MSWD) between 1.7 and 4.3 for all samples.

The most northwesterly sample, 758, came from the biotite-muscovite Sheep Hole Pass Granite. Five of the 10 spot analyses conducted on this sample failed to intersect Tera-Wasserburg concordia and were excluded from the

weighted average age. Zircons from this sample are prismatic to irregular, and the outer approximately one half of many large zircons consists of a CL dark, oscillatory zoned rim, suggesting igneous crystallization with high U concentrations. Analyses in these zones therefore yielded concordant spot ages with errors of ~±0.5 m.y. (Fig. 3). Ages from these zones shifted the overall age toward the older, low-error grains, yielding a weighted average of five grains of 76.5 ± 1.5 Ma, with a high MSWD of 4.3. Due to the weighting of these high U zones, we interpret that this value should be considered a maximum age for sample 758.

Samples 760 and ND45 were collected from outcrops of hornblende-bearing sphene-biotite granodiorite of Clark's Pass. Sample 760 zircons yielded data that are clustered on a Tera-Wasserburg concordia, excepting one grain that was excluded due to large $^{207}Pb/^{235}U$ errors. Ten grains yielded a weighted average of 76.5 ± 1 Ma, with an MSWD of 2.3. Sample ND45 suffered from significant Pb loss, with data spreading along Tera-Wasserburg concordia across ~7 m.y. Four grains significantly younger than the main population were excluded on suspicion of Pb loss. Eight grains yielded a weighted average of 76 ± 1 Ma, with an MSWD of 2.2. Therefore, these two samples of the granodiorite of Clark's Pass yielded comparable ages within error. A nearby sample taken from pink granite associated with pegmatites, sample H12SH-13, yielded significantly younger ages that span from 77 to 65 Ma. A lack of a dominant age population and monotonically decreasing ages in this sample suggest that it was disturbed since formation, experienced significant Pb loss, or contains an unresolvable inherited population, precluding the interpretation of the precise age.

Sample 761 was collected from a large body of predominantly equigranular biotite granite in the central part of the Cadiz Valley batholith, the granite of South Sheep Hole Valley. This sample contained oscillatory zoned zircons that darken toward their rims. The three youngest grains, suspected of Pb loss, were excluded to yield a weighted average age of 75 ± 1 Ma from nine grains, with an MSWD of 1.7, within error of a laser-ablation U-Pb age of 76.1 ± 3.4 Ma reported for a nearby granodiorite (Chapman et al., 2018).

Sample 756 is a muscovite-biotite monzogranite from the Granite Pass Granite pluton, situated east across a broad valley from earlier described samples. This sample contained several discordant grains that indicate common Pb contamination but yielded a coherent age population, excluding one significantly older grain and one significantly younger grain. The remaining 12 grains yielded an age of 74.5 ± 1 Ma, with an MSWD of 1.7. Other studies have reported U-Pb ages of 74.5 ± 2.1 Ma and 71.5 ± 2.8 Ma from this pluton (Wells et al., 2002; Chapman et al., 2018).

## Geochronology of Midcrustal Sheeted Complex Rocks

Zircons from six samples recovered from the Cajon Pass drill hole were analyzed (Fig. 4). Sample CJ133 yielded only Cretaceous grains, with one yielding a significantly older Cretaceous age interpreted to be a premagmatic grain. Seven other grains produced an age of 79 ± 1.5 Ma, with an MSWD of 2.3. Seven grains from sample CJ179 yielded a weighted mean age of 80.5 ± 1 Ma, excluding one significantly younger grain interpreted to have experienced Pb loss. Excluding a single Jurassic grain, CJ395 yielded a weighted mean age of 81 ± 1 Ma, with an MSWD of 1.16 from seven grains. Sample CJ502 contained one grain displaying evidence of Pb loss and two Proterozoic ages that were excluded from the age calculation. Eight zircons yielded an age of 79 ± 1.5 Ma, which was weighted toward the younger end of the population by a number of high-precision, high U grains.

Sample CJ194 yielded eight Jurassic grains and three Cretaceous grains that we interpret to have formed as metamorphic rims based on Th/U ratios >0.1. The main population yielded a weighted mean age of 151 ± 1.5 Ma (MSWD = 0.40). Sample CJ265 contained only Jurassic grains that yielded a weighted mean age of 151 ± 3 Ma, with a high MSWD of 4.8. The high MSWD of this sample is due to the presence of two apparent age populations, the younger of which may have experienced Pb loss.

## Major-Element Geochemistry

Plutons in the study area share common major-element geochemical characteristics as shown on traditional Harker diagrams and follow the calc-alkaline series in A-F-M geochemistry, where A is $Al_2O_3$, F is FeO, and M is MgO (Fig. 6). These plutons transition across the calc-alkalic and alkali-calcic fields in the modified alkali-lime index (MALI) of Frost et al. (2001) and follow the typical magnesian trend of Cordilleran granitoids (Fig. 7). These rocks span the compositional range from metaluminous to weakly peraluminous (Fig. 7).

There are some variations in major elements between units at different crustal levels. The Cadiz Valley batholith is composed of rocks with a compositional range from hornblende-biotite granodiorite to muscovite-biotite granite and from 67 to 74 wt% $SiO_2$. These rocks are dominantly peraluminous and weakly metaluminous, mainly due to elevated $Na_2O$ contents, which rise consistently above the range of compositions defined by mesozonal plutonic rocks. Mesozonal plutons are more compositionally diverse than the Cadiz Valley batholith, including more strongly metaluminous rocks with lower silica contents. Rocks of the sheeted complex are the most compositionally diverse, ranging from 50 to 76% $SiO_2$.

## Trace-Element Geochemistry

REE variations are tightly clustered, lack prominent negative Eu anomalies, and have a moderate middle REE (MREE) depletion and significant heavy REE (HREE) depletion. The Cadiz Valley batholith data yielded average ratios of $La_{(n)}/Yb_{(n)}$ = 15, Dy/Yb = 2.1, and Dy/Dy* = 0.63. Mesozonal samples yielded average ratios of $La_{(n)}/Yb_{(n)}$ = 13, Dy/Yb = 1.8, and Dy/Dy* = 0.55. Sheeted complex samples yielded average ratios of $La_{(n)}/Yb_{(n)}$ = 14, Dy/Yb = 2.5, and Dy/Dy*

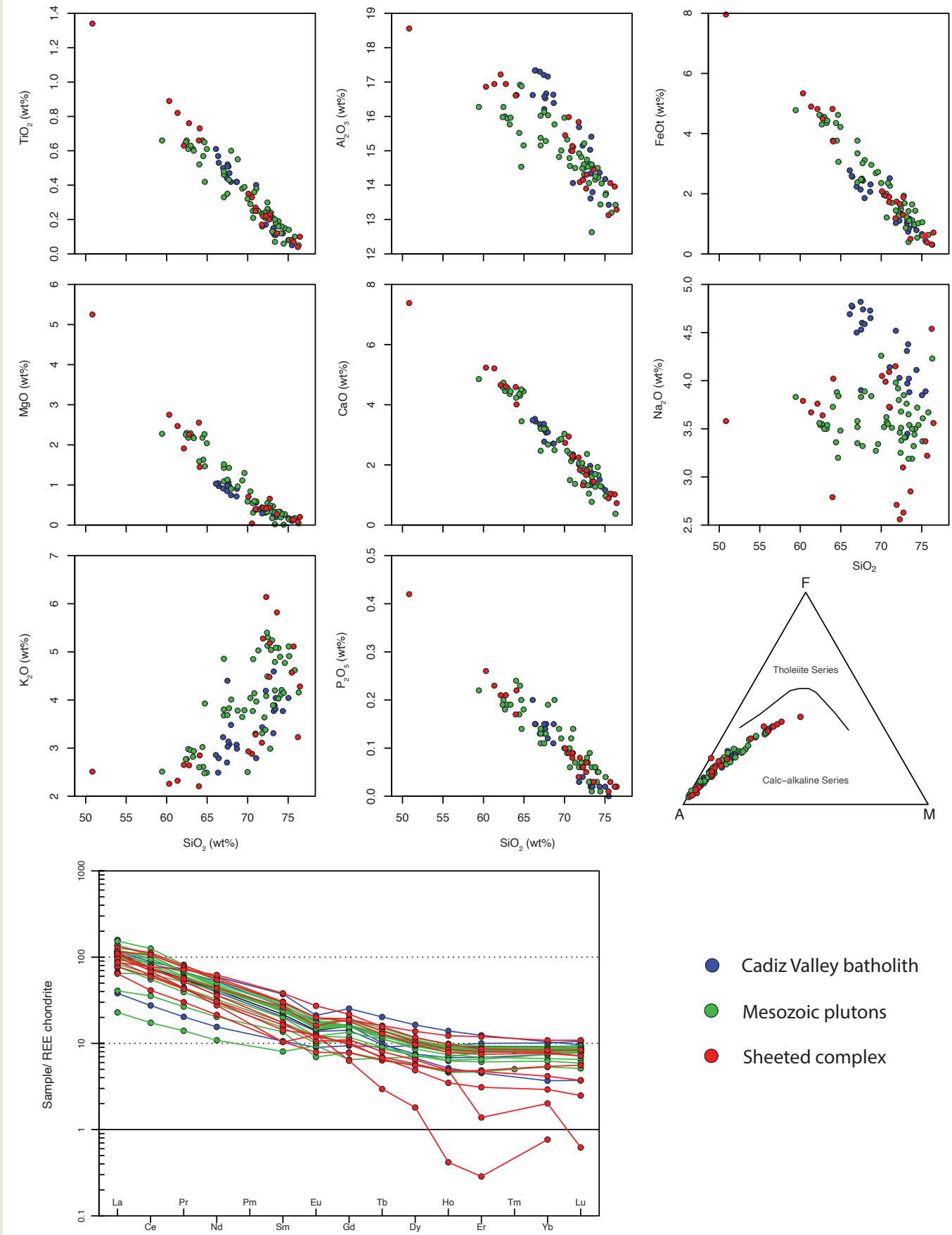


**Figure 6. Harker, AFM (where A is $Al_2O_3$, F is FeO, and M is MgO), and rare earth element (REE) diagrams for igneous rocks in the study area.**

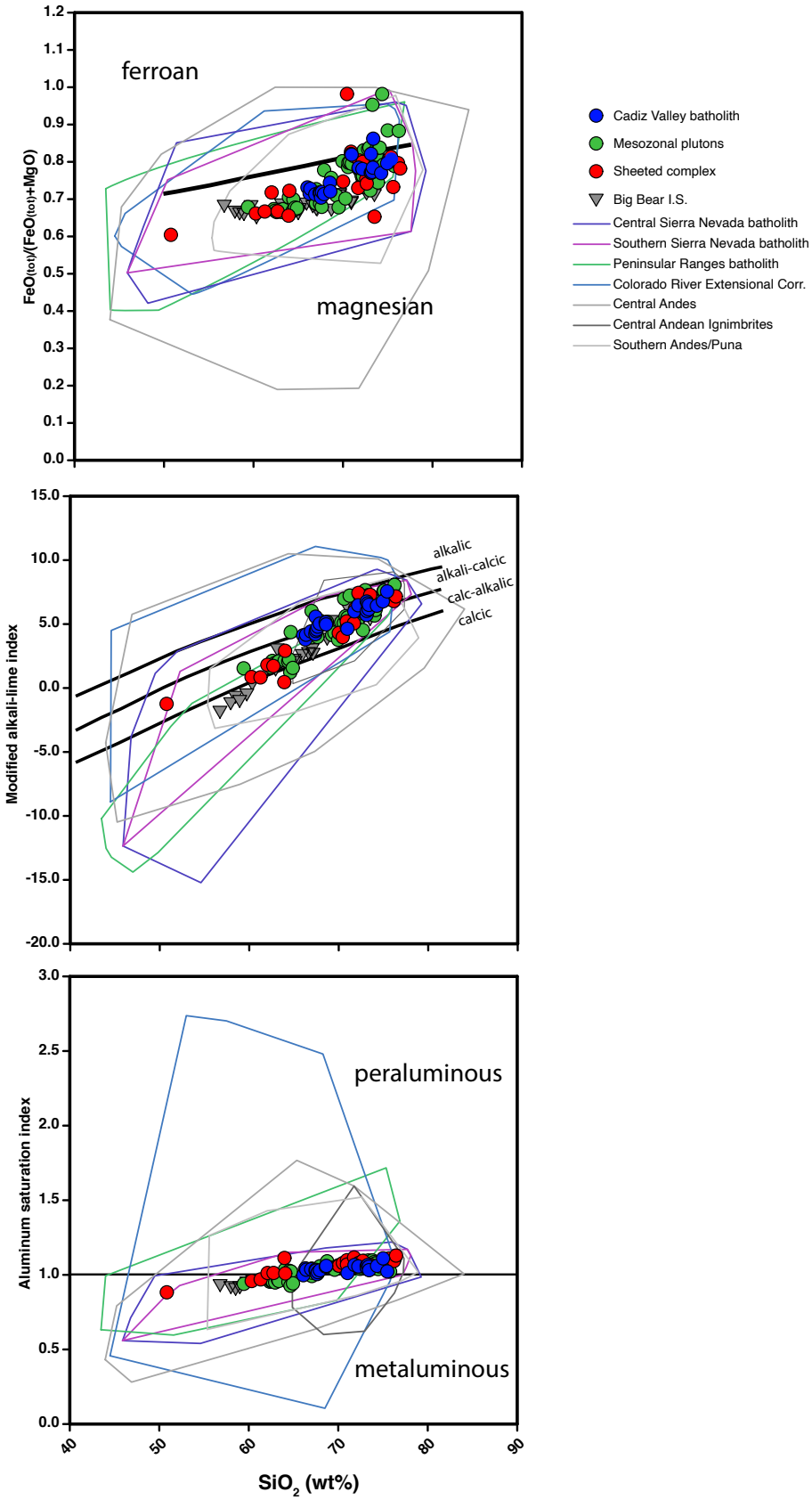


**Figure 7. Aluminum saturation index (ASI), modified alkali lime index (MALI), and Fe number [$FeO_{(total)}$/($FeO_{(total)}$ + MgO)] versus $SiO_2$ for units in the study area as well as the Big Bear intrusive suite (I.S.) (Barth et al., 2016), overlain on fields of several igneous systems for comparison. Data for comparison systems were acquired from North American Volcanic and Intrusive Rock Database (NAVDAT; https://www.navdat.org/), based on parameters indicated, with references in Supplemental Material (see text footnote 1).**

= 0.63 with two outliers removed. Due to the abundance of garnet-bearing host rocks in the sheeted complex, these samples are interpreted as locally contaminated with garnet-bearing material.

All Cadiz Valley batholith samples had Y concentrations of 28 ppm or lower, generally resulting in the highest Sr/Y ratios in the study area, from ~20 to 80 (Fig. 8). The mesozonal plutonic rocks showed a distinctly wider range of Y concentrations, trending toward higher concentrations up to 80 ppm. Sheeted complex compositions largely overlapped with the mesozonal plutons but were distinct from the Cadiz Valley batholith. Concentrations of Y in sheeted complex rocks were nearly ubiquitously higher than those of the Cadiz Valley batholith, and concentrations in the sheeted complex ranged 22–55 ppm (Fig. 8).

Units throughout the region displayed Yb concentrations consistently below 11 ppm and La/Yb ratios generally lower than 60 (Fig. 8). This is in contrast to dichotomous Y concentrations and Sr/Y ratios between Cadiz Valley batholith and sheeted complex samples.

### Rb/Sr and Sm/Nd Isotope Geochemistry

All samples yielded $^{87}Sr/^{86}Sr_{(t)}$ ratios from 0.7075 to 0.7140 and $\varepsilon Nd_{(t)}$ from –10 to –17 (Fig. 9). The $\varepsilon Nd_{(t)}$ and $^{87}Sr/^{86}Sr_{(t)}$ values are negatively correlated. Samples from mesozonal plutons and the sheeted complex overlapped in $\varepsilon Nd_{(t)}$ versus $^{87}Sr/^{86}Sr_{(t)}$ and spanned the entire measured range, whereas Cadiz Valley batholith samples yielded a narrower range of isotopic ratios, with $^{87}Sr/^{86}Sr_{(t)}$ from 0.7097 to 0.7117 and $\varepsilon Nd_{(t)}$ from –12.2 to –14.7.

When all Joshua Tree National Park and Cadiz Valley batholith samples are plotted together, they define a triangular field in $^{87}Sr/^{86}Sr_{(t)}$ versus $SiO_2$ space (Fig. 9) with no distinctive variations between crustal levels beyond the narrower compositional range of the Cadiz Valley batholith. The range of samples with $SiO_2$ ranging from 63 to 76 wt% $SiO_2$ yielded the lowest $^{87}Sr/^{86}Sr_{(t)}$ ratios in the array at ~0.7095, with one outlier diorite from the sheeted complex yielding a ratio of 0.7065. As $SiO_2$ content increases, isotopic diversity also increases, with the most felsic samples yielding a range of $^{87}Sr/^{86}Sr_{(t)}$ from 0.7095 to 0.7135. The range of $^{87}Sr/^{86}Sr_{(t)}$ has no obvious correlation with magmatic age; rather, the range of values is consistent throughout (Fig. 9).

## DISCUSSION

### Regional Age Summary

Samples analyzed from the Cadiz Valley batholith yielded crystallization ages from 76.5 to 74.5 Ma, and a sample from the Coxcomb Mountains yielded a slightly younger age of 73.5 Ma (Barth et al., 2004). Thus, it appears

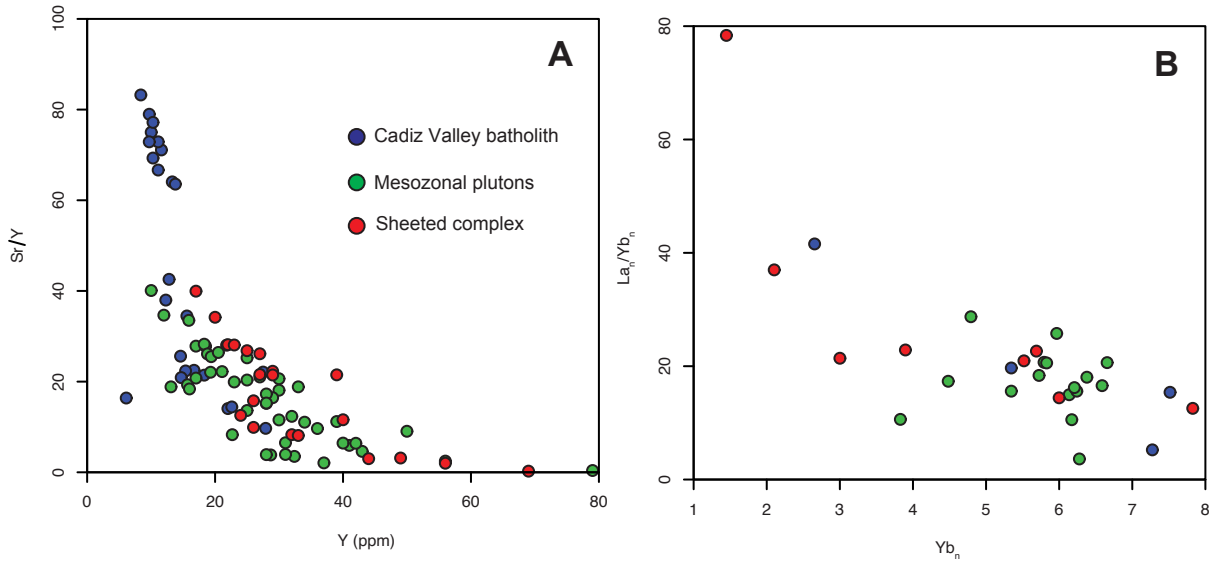


**Figure 8. (A) Sr/Y vs. Y and (B) La/Yb vs. Yb diagrams demonstrating the mismatch in geochemical characteristics for mesozonal plutons and sheeted complex samples for Sr/Y, whereas all samples overlap in La/Yb.**

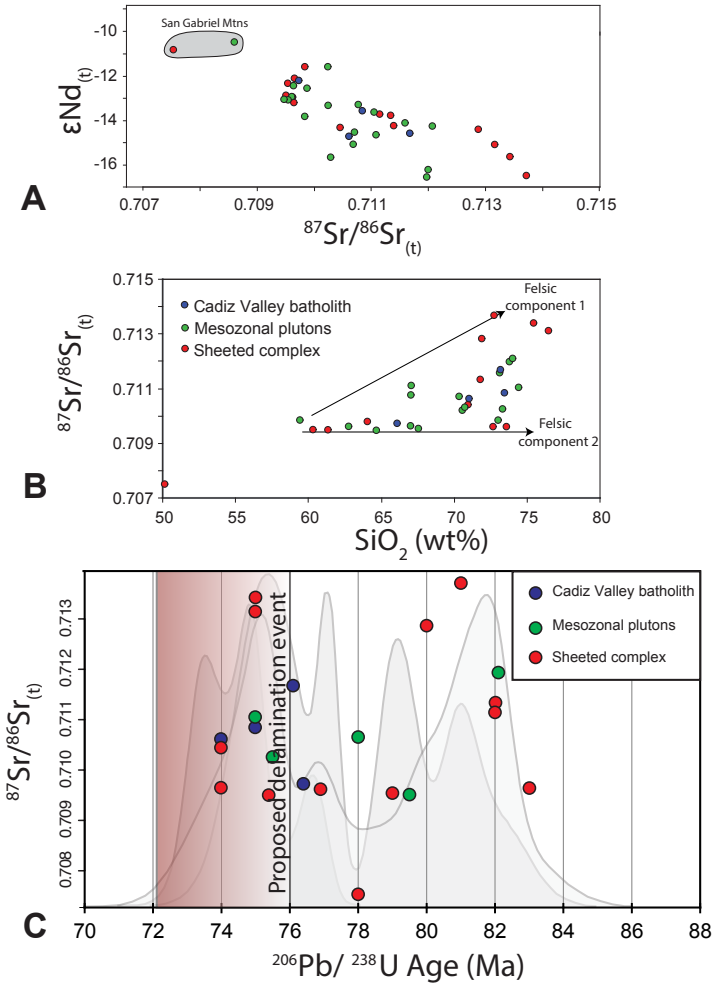


**Figure 9. Whole-rock isotope geochemistry of intrusive rocks from the Eastern Transverse Ranges: (A) Sr and Nd isotopic compositions and the covariation in $\varepsilon Nd_{(t)}$ vs. $^{87}Sr/^{86}Sr_{(t)}$, which follows a negative trend typical for crustally contaminated magmatic bodies. San Gabriel Mountains data are from Barth et al. (1995) and Wiegand et al. (2007). (B) $^{87}Sr/^{86}Sr_{(t)}$ vs. $SiO_2$. Note increasing diversity of $^{87}Sr/^{86}Sr_{(t)}$ in more felsic rocks, and (C) $^{87}Sr/^{86}Sr_{(t)}$ vs. age for all samples in the study with both data sets; age histogram from Figure 5 is plotted in gray for reference.**

that this batholith was emplaced largely over an ~3 m.y. time span. Samples from the Cajon Pass drill hole indicate that the sheeted, heterogeneous plutonic unit in this region contains components of both Late Jurassic and 81–79 Ma ages.

A compilation of new and published SIMS ages of magmatic rocks in the central and Eastern Transverse Ranges establishes overlapping age peaks in both the Late Jurassic and Late Cretaceous across a range of crustal depths. Figure 5 includes data from the Cadiz Valley batholith, mesozonal plutons, and sheeted complex intrusions from Joshua Tree National Park (Barth et al., 2004; Needy et al., 2009; Friesenhahn, 2018), the Big Bear Lake intrusive suite in the San Bernardino Mountains (Barth et al., 2008, 2009), and samples from the Cajon Pass drill core. Cretaceous plutons in the Joshua Tree National Park and the central Mojave Desert were intruded over a time span of ~11 m.y., from ca. 83 to 73.5 Ma. Magmatism occurred in two apparent pulses, one from 83 to 78 Ma and another from 76 to 73.5 Ma. The first pulse formed sheets and mesozonal plutons, synchronous with the intrusion of the Big Bear Lake intrusive suite and Cajon Pass sheeted complex. The second pulse formed sheets, mesozonal plutons, and the Cadiz Valley batholith.

Friesenhahn (2018) found similar and slightly older ages of ca. 88–84 Ma in the deepest exposed plutons in Wide Canyon, coincident with pluton ages in the Teutonia batholith in the central Mojave Desert and in the San Gabriel Mountains (Barth et al., 2004, 2016). The intrusion of all of these bodies represents a Cretaceous pulse of mid- to upper-crustal magmatism, which falls into the shorter end of the typical duration of flare-up events as described by Paterson et al. (2011).

The presence of these igneous materials presents a significant conflict with the purported cessation of all magmatism in the "Southern California batholith" by ca. 85 Ma (Liu et al., 2010). In fact, most Late Cretaceous igneous intrusions in the Eastern Transverse Ranges and central Mojave area were emplaced between 83 and 73.5 Ma.

## Regional Correlations

Needy et al. (2009) proposed that the exposure of plutons in Joshua Tree National Park represents a cross section of the Mojave crust, with an apparent homoclinal dip of ~8° for most of its length, with tilting steepening close to the San Andreas fault (Powell, 1981; Needy et al., 2009; Ianno, 2015; Friesenhahn, 2018). The projection of this 8° dip eastward into the central Mojave Desert would fit well with the published intrusion depth estimate of ~6 km for the Cadiz Valley batholith (Anderson, 1988). Commonalities between the plutons in Joshua Tree National Park and the Cadiz Valley batholith support its inclusion in this oblique cross section, including synchronous intrusion ages and overlapping major-element and isotopic compositional characteristics. Within this region, brittle strain due to active tectonism in southern California is distributed on a myriad of structures that are small relative to the scope of the cross section. We propose that the Eastern Transverse Ranges–central

Mojave Desert tilted crustal section should be considered as bounded in the east (shallowest) by the breakaway of the Colorado River extensional corridor (Howard and John, 1987; Faulds et al., 2001) and in the west (deepest) by the San Andreas fault. We further project this cross section to the northwest to encompass the Big Bear Lake intrusive suite and the underlying sheeted rocks sampled in the Cajon Pass drill core.

The shallowest exposures at 5–6 km paleodepth and the midcrustal exposures at ~18–20 km paleodepth are ~80 km apart perpendicular to the paleo–continental margin, and so the plutons in this cross section cannot be directly correlated. Rather, they are representative of the various levels of the crust in the Mojave region during Late Cretaceous magmatism. The following discussion therefore requires the caveat that variations between units in the section may be attributable to either variations with depth or regional variations perpendicular to the paleo–continental margin.

The interpretation that these igneous bodies are part of a coherent, albeit strongly oblique, crustal section is supported by an indistinguishable range of Sr and Nd isotopic compositions among all intrusions, excepting that the Cadiz Valley batholith displays a tighter compositional range that falls within that defined by the more diverse sheeted complex. We interpret the sheeted complex to have been constructed of smaller-volume aliquots that are representative of the diversity of source components for mesozonal and upper-crustal plutons. The $\varepsilon Nd_{(t)}$ and $^{87}Sr/^{86}Sr_{(t)}$ values overlap with isotope values from deeply intruded Cretaceous plutons from the San Gabriel Mountains (Fig. 9; Barth et al., 1995; Wiegand et al., 2007). The isotopically similar source materials of regional plutonism are likely due to the widespread presence of Proterozoic basement throughout the crust in the Mojave Desert as a fertile source for material addition to the Cretaceous magmatic system, as is envisaged for other sectors of the Cordilleran arc system (Ducea, 2001). Additional support for abundant incorporation of Proterozoic source material in these rocks comes from the ages of inherited zircons (Tables S1 and S2 [footnote 1]) and from Pb isotope studies (Wooden et al., 2018).

Furthermore, the along-strike (NW/SE) spatial extent of the sheeted complex, in the Little San Bernardino Mountains, San Bernardino Mountains, and the Cajon Pass drill hole, suggests that this major feature observed in the midcrust was regionally extensive, at least as exposed along strike of the paleo–continental margin. Evidence for a correlation between the sheeted complex in Joshua Tree National Park and rocks sampled by the Cajon Pass drill core includes similarities in large-scale and small-scale sheeted structural characteristics, intrusive depths corresponding to ~4–6 kbar, a similar breadth of compositions, dominantly magmatic fabrics, and both Jurassic and Cretaceous ages that overlap within analytical error. This correlation implies that the sheeted complex is laterally extensive over >100 km along strike to the northwest and everywhere that sufficient depths are exposed.

First-order variations from western midcrustal to eastern shallow crustal intrusions include the following:

- increasing major- and trace-element homogeneity (which may mask the apparent sizes of magmatic pulses in the shallow crustal plutons);
- increasing apparent magmatic pulse volume from a complex of small sheets and sills to moderately sized composite plutons at mesozonal levels to a vast granitic to granodioritic batholith in the shallow crust;
- decreasing abundance of the more mafic compositions, leading to an overall higher average $SiO_2$ content; and
- decreasing abundance of older magmatic units (ages of ca. 83–76 Ma), where the sheeted complex and mesozonal plutons span the age range ca. 83–73.5, whereas the upper-crustal Cadiz Valley batholith yields only 76.5–73.5 Ma ages.

## Is Geochemistry Consistent with Arc Magmatism?

Late Cretaceous igneous rocks in the study area display all of the geochemical hallmarks of arc magmatism, including a calc-alkaline compositional trajectory and metaluminous to peraluminous compositions. These characteristics are common in evolved arc magmas that intrude a thickened crust, such as the Andean arc and the Sierra Crest event of the Sierra Nevada batholith (Coleman and Glazner, 1997; shown for comparison in Fig. 7). Indeed, major-element variations such as aluminosity and total alkali content are indistinguishable between Mojave igneous rocks and granitoids of the central and southern Sierra Nevada batholith, eastern Peninsular Ranges batholith, and the central Andean arc (Fig. 7). Behaviors of these magmas on a modified alkali lime index (Fig. 7) cross from the calc-alkalic to the alkali-calcic field, which broadly suggests contamination with a heterogeneous crustal source, as is evident from the Proterozoic to early–middle Mesozoic geology of the Transverse Ranges and the Mojave Province.

Whole-rock REE patterns may record the influence of mineral fractionation in the deeper, unexposed portions of a magmatic system on evolved, shallowly emplaced magmatic products (e.g., Davidson et al., 2007, 2013). REE patterns from rocks in this study show progressive MREE and HREE depletions, yielding steep REE patterns with average La/Yb ratios for each crustal level in the range of ~13–15 (excluding two strong outliers in the sheeted complex). Calculated ratios of Dy/Dy* range from ~0.55 to 0.63, indicating a mild but significant downward inflection of the MREEs. These observations are generally consistent with the fractionation and/or removal of both garnet and hornblende in the deep crust of the magmatic system, although these patterns may also be influenced by later-crystallizing accessory phases. The lack of a prominent negative Eu anomaly indicates either a lack of strong plagioclase fractionation or an oxidized magmatic source, as is expected for arc magmas.

All samples in the region are considered to be isotopically evolved relative to plutons of similar age elsewhere in the Mesozoic California arc (e.g., Kistler and Ross, 1990), likely due to the incorporation of an older Proterozoic crustal component in this region. Geochemistry indicates multiple stages of contamination of a complex crustal source, as is typical of arc magmatic systems. The $^{87}Sr/^{86}Sr_{(t)}$ values for samples from the sheeted complex with $SiO_2$ contents as low as 60 wt% are ~0.709, indicating that crustal contamination has already

played a role in the formation of these mafic to intermediate granitoids (Fig. 9). Data suggest that a crustal component of $^{87}Sr/^{86}Sr_{(t)}$ = 0.714 or higher participated in additional crustal contamination, and granites that range down to $^{87}Sr/^{86}Sr_{(t)}$ = 0.709 may have been influenced by multiple crustal components, fractionation, or both. It is not possible to unequivocally differentiate between the effects of crustal contamination or the control of an isotopically enriched mantle source region because no primary mafic compositional end members have been identified.

However, it is clear that there is no geochemical distinction between 88 and 85 Ma intrusions and 76–73.5 Ma intrusions in either bulk chemistry (Fe#, alumina saturation index [ASI], or MALI; Fig. 7) or isotopic signature (Fig. 9), beyond a trend toward overall more felsic compositions. One would expect to observe some changes in these geochemical parameters over time in the scenario of a foundering lower crust and asthenospheric melt ingress as a driver for batholithic-scale magmatism (Wells and Hoisch, 2008; Hildebrand and Whalen, 2017), particularly if the mantle lithosphere exerts a critical control on the isotopic state of igneous products (Chapman et al., 2017, 2018). For example, in the Himalayan Gangdese batholith, a swarm of mafic magmatism with primitive isotopic characteristics accompanied delamination and/or slab break-off (Dong et al., 2005; Ji et al., 2012). Lacking any evidence of a heat source from upwelling asthenospheric mantle, arc magmatism is the likeliest formation environment.

Traditional trace-element characteristics designed to discriminate tectonic environment (e.g., Pearce et al., 2005) are of limited utility in evolved and heavily contaminated igneous rocks such as those in the study area. Crustal anatexis and hybridization perturb elements such as Y, Yb, and Rb by interaction with garnet-bearing biotite gneissic host rocks and Th and Zr through copious zircon inheritance. Concentrations of fluid-immobile high field strength elements such as Ta and Nb tend to be depleted in magmas generated in arc settings. However, concentrations of these elements are not appreciably different between Sierran granitoids, Mojave granitoids, and those of the Colorado River extensional corridor, suggesting that these elemental ratios, like isotopic ratios, may be controlled by lithospheric sources rather than subduction dynamics (e.g., Chapman et al., 2017).

## Is There Evidence for a Reduction in Crustal Thickness between 82 and 74 Ma?

In addition to predicted shifts in elemental and isotopic geochemistry, a delamination event may trigger a reduction in crustal thickness, e.g., depth to Moho, while ongoing arc magmatism would predict persistence of a thick crust throughout the time period of Eastern Transverse Ranges and Mojave plutonism. Concentrations of Sr, Y, and Sr/Y ratios are commonly used to evaluate the mineralogical constituents of source regions, particularly the predominance of plagioclase (which strongly partitions Sr) and garnet (which strongly partitions Y), although amphibole may play a significant role in MREE/HREE fractionation (Davidson et al., 2007). A prevalence of garnet over plagioclase in the source region would be suggestive of melting deeper than ~35 km (Kay and Kay, 1993; Macpherson et al., 2006). High Y concentrations imply that garnet was not a significant residual phase; therefore, magmas were generated either outside of the garnet stability field for lower-crustal I type sources (less than ~35 km) or from S-type sources that underwent garnet breakdown and therefore liberated Y into the melt. The ratios of light to heavy REEs (LREE/HREE), specifically La/Yb, are also considered as an indicator of the involvement of garnet in the source based on the preferential partitioning of HREEs therein.

The low Y concentration and therefore high Sr/Y ratios in all Cadiz Valley batholith magmas implicate a garnet-bearing source for the Cadiz Valley batholith magmas (Fig. 8). The ratios of La/Yb are also indicative of the presence of garnet in the source region, with high La/Yb ratios and low Yb concentrations. We used the empirical calibration of Profeta et al. (2015) to examine paleocrustal thickness across the region. Data were filtered using the protocol described therein, except that a lower MgO concentration cutoff (0.9 vs. 1.0) was used to capture more samples in the estimate. More felsic samples were also included in the Cadiz Valley batholith $La/Yb_{(n)}$ estimate due to a low total number of data points, but the $La/Yb_{(n)}$ estimates generally should be less sensitive to filtering, as is indicated by relatively consistent values between filtered and unfiltered data (Fig. 10). No outliers were removed. Crustal thickness estimates yielded broadly consistent results for the Cadiz Valley batholith, with both Sr/Y and $La/Yb_{(n)}$ indicating a thick crust during magmatism (Fig. 10). Rocks of similar ages and overlapping trace-element compositional characteristics from the San Gabriel Mountains suggest that this is a regionally consistent finding (Barth et al., 1995; Paterson et al., 2017).

However, Sr/Y and $La/Yb_{(n)}$ ratios yielded conflicting results for mesozonal and sheeted complex samples. Sr/Y ratios from mesozonal and sheeted complex samples indicate thin crust, while $La/Yb_{(n)}$ ratios indicate thick crust. Possible causes for the inconsistency in these ratios could be the geochemical influence of midcrustal metamorphic Proterozoic units, which contain abundant garnet. Garnet-rich schists and granulites that are locally interleaved with sheeted complex rocks have extreme Y concentrations, up to 160 ppm (A. Barth, personal commun., 2018). These units are a likely candidate for perturbation of Y/Yb in adjacent magmatic units due to the interleaved, high-temperature contacts between Proterozoic and Cretaceous intrusive units. There is abundant field evidence for interaction between Proterozoic units and adjacent Cretaceous magmatic sheets, including copious lit par lit intrusion and local migmatization of Proterozoic framework rocks and abundant inherited Proterozoic zircons found in nearly all Cretaceous samples in the entire region (e.g., Needy et al., 2009; this study). Ratios of Y/Yb from mesozonal and sheeted complex rocks are anomalous in comparison with other arc-magmatic systems (Fig. 11). Ratios of Y/Yb may be useful indicators of the geochemical influence of garnet grown in regional metamorphic events on magmatic products, but more development is needed.

$La/Yb_{(n)}$ ratios for all crustal levels in the study area give a coherent indication that magmas were generated in a thickened continental crust. Based on variations in Y behavior in midcrustal plutonic and host rocks, Sr/Y ratios more

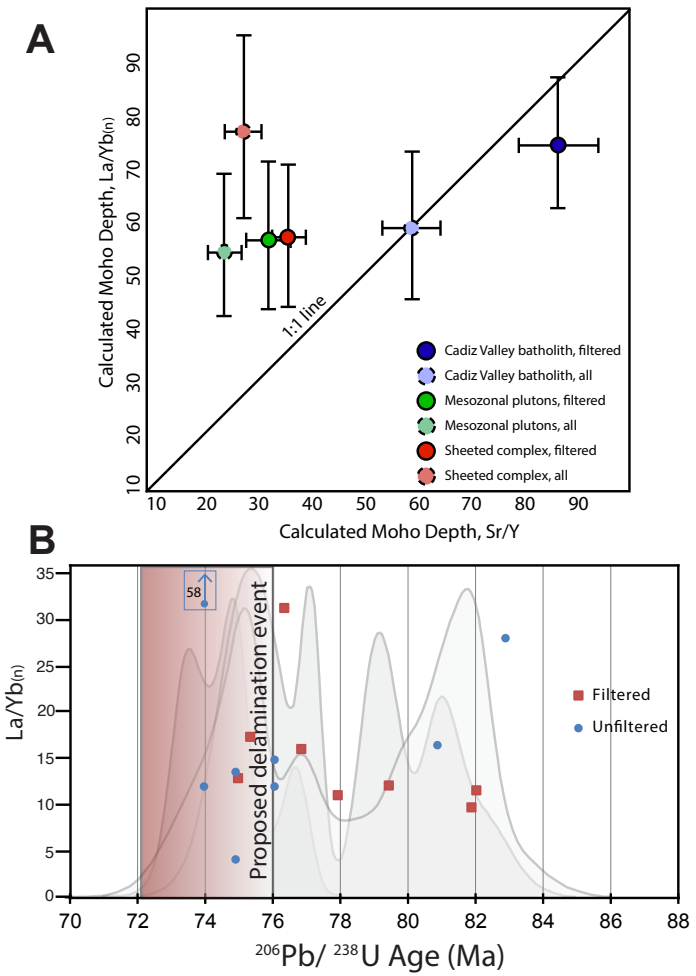


**Figure 10. (A) Comparison of calculated "depth to Moho" from Sr/Y and La/Yb$_{(n)}$ ratios for rocks from the Cadiz Valley batholith, mesozonal plutons, and the sheeted complex utilizing the empirical formulation of Profeta et al. (2015) for data that were filtered according to the Profeta et al. (2015) protocol (solid symbols) and all data (dashed symbols). Note that the Cadiz Valley batholith yields consistent values for depth, while mesozonal plutons and sheeted complex rocks yield significantly shallower depths for Sr/Y than La/Yb. (B) La/Yb$_{(n)}$ vs. age for all samples in the study with both data sets; age histogram from Figure 5 is plotted in gray for reference.**

likely reflect overlapping influence of deep residual garnet and local plutonic interactions with midcrustal garnet-bearing schists and gneisses. We therefore favor the depth interpretation from La/Yb$_{(n)}$ ratios that suggest the crust was thick at the time that the Cretaceous magmatic column was constructed. The interpretation of a thick crust in Cretaceous time is in good agreement with the broader tectonic (Livaccari, 1991) and regional geologic context. Deep crustal exposures in the San Gabriel Mountains restore palinspastically to this geographic region (Powell, 1993; Matti and Morton, 1993).

## Tectonic Setting

Current conceptualizations of the underthrusting of the Shatsky Rise conjugate below North America require its insertion beneath a relatively narrow zone between the Sierra Nevada batholith and the Peninsular Ranges batholith, followed by a more northeasterly trajectory of underthrusting beneath central-western North America (e.g., Liu et al., 2010). Our trace-element data and regional geology suggest that the magmas that produced the studied plutons passed through a thick crust. Friesenhahn (2018) demonstrated, based on synmagmatic deformation features, that the midcrustal rocks in the Little San Bernardino Mountains preserve contractional structures, although there is ample evidence for synmagmatic mid- to upper-crustal extension in the eastern Mojave area (McCaffrey et al., 1999; Wells et al., 2005; Wells and Hoisch, 2008). Furthermore, the monotonic nature of the most primitive isotopic ratios preserved primarily in the sheeted complex does not agree with a shift from a subduction to a delamination setting in the Late Cretaceous, as there is no isotopic deflection to lower $^{87}Sr/^{86}Sr_{(i)}$ (Fig. 9) compositions as would be expected to accompany the influx of asthenospheric melts and no deflection in La/Yb$_{(n)}$ (Fig. 10) that would indicate a change in crustal thickness.

Magmatism with calc-alkaline compositions intruding a thickened crust during tectonic compression is the simplest to explain as arc magmatism. Xenoliths from central Arizona, hypothesized to be lower-arc crust derived from the Mojave at ca. 75 Ma, corroborate this interpretation (Chapman et al., 2020a). Following this line of reasoning, the Late Cretaceous igneous rocks in the Mojave Desert are not so unlike all of the other plutons of Late Cretaceous age in the Sierra Nevada batholith, although the Mojave magmatic pulse was apparently smaller and ~10 m.y. younger (Paterson et al., 2011).

One caveat is the trench-perpendicular width of magmatism in the Eastern Transverse Ranges and central Mojave area. The described composite crustal section has a very shallow angle, and mesozonal and sheeted complex rocks are 80 km west of the center of the Cadiz Valley batholith. This geometry is only achievable if the arc was actively migrating eastward at this time, as has been proposed by other workers (e.g., Chapman et al., 2018). Eastward migration of the locus of magmatism is corroborated by ages in both the sheeted complex and the Big Bear Lake intrusive suite, which are older than the more easterly Cadiz Valley batholith (Fig. 5; Barth et al., 2016). This eastward arc migration is a key component of the model of Jones et al. (2011), which hypothesizes that

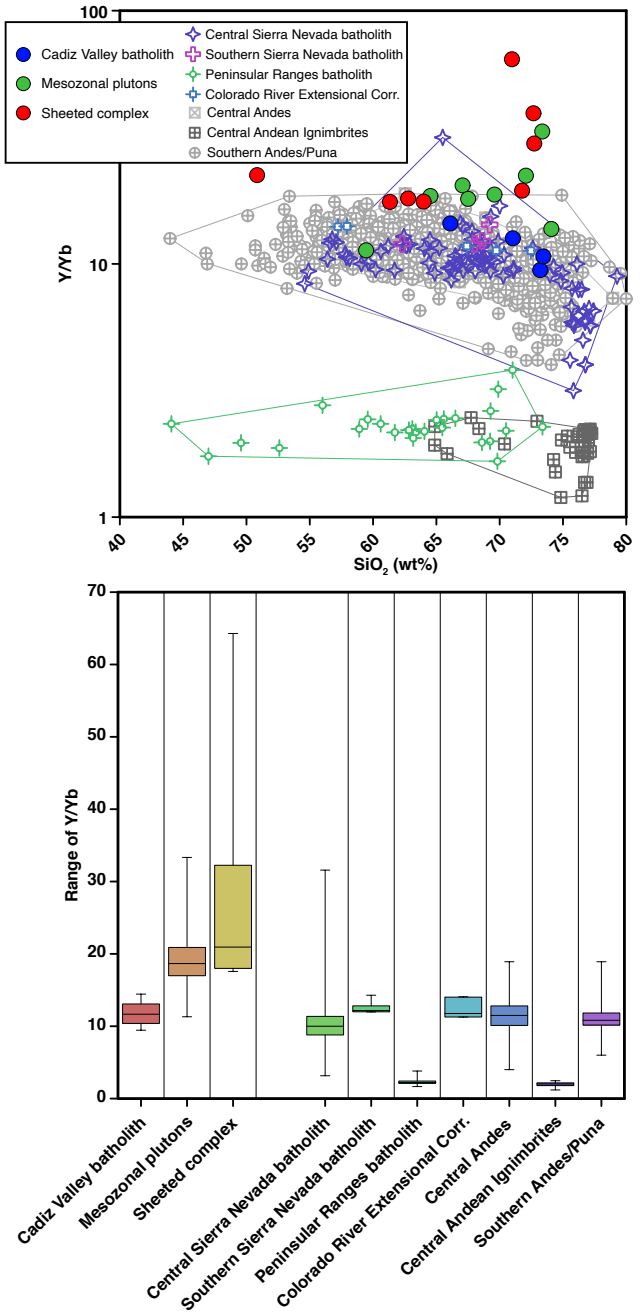


**Figure 11. Y/Yb for rocks from the study area and several igneous systems for comparison. (Data were acquired from North American Volcanic and Intrusive Rock Database [NAVDAT; https://www.navdat.org/] based on parameters indicated in Supplemental Material [text footnote 1].) Plots show that mesozonal plutons and sheeted complex samples yield anomalously high Y/Yb ratios, leading to the mismatch between the results of different depth calculations.**

a moderately shallowing slab interacted with the Wyoming craton to transfer deformation inboard without the transit of a "flat" slab into the continental interior beneath the Mojave region. This model accommodates all of our observations in that it allows for the synchronicity of arc magmatism in the Mojave region and inboard deformation in Wyoming, shortly followed by the underplating of forearc sedimentary units. Our findings are also consistent with the proposed timing of the passage of a shallowly dipping slab (Hess Rise conjugate?) beneath the Mojave region at ca. 65 Ma (e.g., Chapman et al., 2020b), and they are in good agreement with more recently proposed reconstructions based on the presence of Laramide-aged lithospheric xenoliths from central Arizona that were likely endemic to the Mojave region (Chapman et al., 2020a).

Multiple potentially germane magmatic-tectonic events occurred shortly before or synchronous with the events described herein for the Eastern Transverse Ranges and central Mojave. These include magmatism associated with crustal thickening in the Ruby and Humboldt Ranges in Nevada behind the Sierra Nevada batholith at ca. 90 and ca. 80 Ma (Lee et al., 2003; Arendale et al., 2011; Howard et al., 2011; Chapman et al., 2015). However, magmatism of the same age in Nevada is of distinctly different character, being strongly peraluminous and a product of dominantly local crustal melting with no associated mafic intrusions (Lee et al., 2003).

The Salinian block is reconstructed to the north and outboard of the regions addressed in this paper (Chapman et al., 2012). Magmatism there extended from the early–mid-Cretaceous through ages that overlap with the plutons studied here (Kidder et al., 2003). Based on detailed structural and geochronological studies in the Salinian block, the southern Sierra Nevada batholith was undergoing extensional collapse between ca. 80 and 70 Ma, while magmatism continued in the central Mojave (Schott and Johnson, 1998; Barth et al., 2003; Kidder and Ducea, 2006; Chapman et al., 2012). Although the sequence of events in Salinia is very similar to that in the Mojave (plutonism, schist emplacement, and extensional collapse), the time line is consistently older in Salinia. Additional work on Cretaceous igneous intrusions from the north-central Mojave may shed some light on the nature of the crustal transition between these two provinces.

## CONCLUSIONS

New and existing geochronology and geochemistry data corroborate and expand the scope of the Transverse Ranges tilted crustal section to include the

Cadiz Valley batholith of the Mojave Desert and intrusive rocks in the San Bernardino Mountains. Isotope geochemistry indicates a common heterogeneous crustal source for Cretaceous magmatic units at shallow and midcrustal levels in the Mojave Desert. We observed no significant geochemical deflections that would indicate asthenospheric ingress or change in crustal thickness during magmatism. Major-element geochemistry of these rocks is consistent with formation in an arc environment. Trace-element geochemistry also contains complications but suggests that the Cretaceous magmatic system in the study region formed in a thickened continental crustal column, which, along with indications of compressional midcrustal features in the Little San Bernardino Mountains from Friesenhahn (2018), is best explained by a subduction environment. This conclusion is permissive of the ca. 75–65 Ma timing for exhumation and flat-slab passage through the Mojave region but in conflict with a tectonic model of flat-slab subduction of the conjugate Shatsky Rise at ca. 85 Ma beneath this portion of the Cordilleran arc. Significant volumes of Late Cretaceous magmatism were continuous throughout the transition from Sevier to Laramide orogenesis and must factor into any model of the geological evolution of this region. We consider this magmatism as a critical record of the evolution of the Mojave segment of the continental margin in Late Cretaceous time.


## ACKNOWLEDGMENTS

This work was supported by National Science Foundation grants EAR-0711119 and EAR-0809003 awarded to Barth and by Southern Methodist University, and it was made possible by field support from the National Park Service. Special thanks go to Luke Sabala and the Joshua Tree National Park rangers. We thank Robert Powell, Jay Chapman, and Scott Johnson for thoughtful reviews, and Lang Farmer for his editorial expertise. We thank Carl Jacobson and Jane Pendrick for their expert assistance with zircon separations, Michelle Gevedon for insightful discussions, and Brad Ito for long-time expert maintenance of the Stanford ion microprobe.


## REFERENCES CITED


Anderson, J.L., 1988, Core complexes of the Mojave-Sonoran Desert: Conditions of plutonism, mylonitization, and decompression, *in* Ernst, W.G., ed., Metamorphism and Crustal Evolution of the Western United States: Englewood Cliffs, New Jersey, Prentice Hall, p. 503–525.

Anderson, J.L., and Bender, E.E., 1989, Nature and origin of Proterozoic A-type magmatism in the southwestern United States of America: Lithos, v. 23, p. 19–52, https://doi.org/10.1016/0024-4937(89)90021-2.

Anderson, J.L., and Morrison, J., 1992, The role of anorogenic granites in the Proterozoic crustal development of North America, *in* Condie, K.C., ed., Proterozoic Crustal Evolution: Amsterdam, Netherlands, Elsevier, Developments in Precambrian Geology 10, p. 263–299, https://doi.org/10.1016/S0166-2635(08)70121-X.

Arendale, A.H., Hetherington, C.J., Cottle, J.M., and Barnes, C.G., 2011, Constraining the onset of Cretaceous peraluminous magmatism in the Ruby Mountains, Nevada: Geological Society of America Abstracts with Programs, v. 43, no. 4, p. 14, https://gsa.confex.com/gsa/2011RM/webprogram/Paper187532.html.

Barth, A.P., 1990, Mid-crustal emplacement of Mesozoic plutons, San Gabriel Mountains, California, and implications for the geologic history of the San Gabriel terrane, *in* Anderson, J.L., ed., The Nature and Origin of Cordilleran Magmatism: Geological Society of America Memoir 174, p. 33–456, https://doi.org/10.1130/MEM174-p33.

Barth, A.P., and Dorais, M.J., 2000, Magmatic anhydrite in granitic rocks: First occurrence and potential petrologic consequences: The American Mineralogist, v. 85, p. 430–435, https://doi.org/10.2138/am-2000-0404.

Barth, A.P., and May, D.J., 1992, Mineralogy and pressure-temperature-time path of Cretaceous granulite gneisses, southeastern San Gabriel Mountains, southern California: Journal of Metamorphic Petrology, v. 10, p. 529–544, https://doi.org/10.1111/j.1525-1314.1992.tb00103.x.

Barth, A.P., and Schneiderman, J.S., 1996, A comparison of structures in the Andean orogen of northern Chile and exhumed midcrustal structures in southern California, USA: An analogy in tectonic style?: International Geology Review, v. 38, p. 1075–1085, https://doi.org/10.1080/00206819709465383.

Barth, A.P., and Wooden, J.L., 2006, Timing of magmatism following initial convergence at a passive margin, southwestern U.S. Cordillera, and ages of lower crustal magma sources: The Journal of Geology, v. 114, p. 231–245, https://doi.org/10.1086/499573.

Barth, A.P., Wooden, J.L., and May, D.J., 1992, Small scale heterogeneity of Phanerozoic lower crust: Evidence from isotopic and geochemical systematics of mid-Cretaceous granulite gneisses, San Gabriel Mountains, southern California: Contributions to Mineralogy and Petrology, v. 109, p. 394–407, https://doi.org/10.1007/BF00283327.

Barth, A.P., Wooden, J.L., Tosdal, R.M., and Morrison, J., 1995, Crustal contamination in the petrogenesis of a calc-alkaline rock series: Josephine Mountain intrusion, California: Geological Society of America Bulletin, v. 107, p. 201–212, https://doi.org/10.1130/0016-7606(1995)107<0201:CCITPO>2.3.CO;2.

Barth, A.P., Tosdal, R.M., Wooden, J.L., and Howard, K.A., 1997, Triassic plutonism in southern California: Southward younging of arc-initiation along a truncated continental margin: Tectonics, v. 16, no. 2, p. 290–304, https://doi.org/10.1029/96TC03596.

Barth, A.P., Wooden, J.L., Grove, M., Jacobson, C.E., and Pendrick, J.N., 2003, U-Pb zircon geochronology of rocks in the Salinas Valley region of California: A reevaluation of the crustal structure and origin of the Salinia block: Geology, v. 31, no. 6, p. 517–520, https://doi.org/10.1130/0091-7613(2003)031<0517:UZGORI>2.0.CO;2.

Barth, A.P., Wooden, J.L., Jacobson, C.E., and Probst, K., 2004, U-Pb geochronology and geochemistry of the McCoy Mountains Formation, southeastern California: A Cretaceous retroarc foreland basin: Geological Society of America Bulletin, v. 116, p. 142–153, https://doi.org/10.1130/B25288.1.

Barth, A.P., Wooden, J.L., Howard, K.A., and Richards, J.L., 2008, Late Jurassic plutonism in the southwest U.S. Cordillera, *in* Wright, J.E., and Shervais, J.W., eds., Arcs, Ophiolites and Batholiths: A Tribute to Cliff Hopson: Geological Society of America Special Paper 438, p. 379–396, https://doi.org/10.1130/2008.2438(13).

Barth, A.P., Wooden, J.L., Coleman, D.S., and Vogel, M.B., 2009, Assembling and disassembling California: A zircon and monazite geochronologic framework for Proterozoic crustal evolution in southern California: The Journal of Geology, v. 117, p. 221–239, https://doi.org/10.1086/597515.

Barth, A.P., Wooden, J.L., Mueller, P.A., and Economos, R.C., 2016, Granite provenance and intrusion in arcs: Evidence from diverse zircon types in Big Bear Lake intrusive suite, USA: Lithos, v. 24–247, p. 261–278, https://doi.org/10.1016/j.lithos.2015.12.009.

Barth, A.P., Wooden, J.W., Miller, D.M., Howard, K.A., Fox, L.K., Schermer, E.R., and Jacobson, C.E., 2017, Regional and temporal variability of melts during a Cordilleran magma pulse: Age and chemical evolution of the Jurassic arc, eastern Mojave Desert, California: Geological Society of America Bulletin, v. 129, p. 429–448, https://doi.org/10.1130/B31550.1.

Bird, P., 1998, Kinematic history of the Laramide orogeny in latitudes 35°–49°N, western United States: Tectonics, v. 17, no. 5, p. 780–801, https://doi.org/10.1029/98TC02698.

Black, L.P., Kamo, S.L., Allen, C.M., Davis, D.W., Aleinikoff, J.N., Valley, J.W., Mundil, R., Campbell, I.H., Korsch, R.J., Williams, I.S., and Foudoulis, C., 2004, Improved $^{206}Pb/^{238}U$ microprobe geochronology by the monitoring of a trace-element-related matrix effect, SHRIMP, ID-TIMS, ELA-ICP-MS and oxygen isotope documentation for a series of zircon standards: Chemical Geology, v. 205, p. 115–140, https://doi.org/10.1016/j.chemgeo.2004.01.003.

Calzia, J.P., 1982, Geology of granodiorite in the Coxcomb Mountains, southeastern California, *in* Frost, E.G., and Martin, D.L., eds., Mesozoic–Cenozoic Tectonic Evolution of the Colorado River Region, California: San Diego, California, Cordilleran Publishers, p. 173–180.

Calzia, J.P., DeWitt, E., and Nakata, J.K., 1986, U-Th-Pb age and initial strontium isotopic ratios of the Coxcomb granodiorite and a K-Ar date of olivine basalt from the Coxcomb Mountains, southern California: Isochron-West, v. 47 p. 3–8.

Chapman, A.D., Saleeby, J.B., Wood, D.J., Piasecki, A., Kidder, S., Ducea, M.N., and Farley, K.A., 2012, Late Cretaceous gravitational collapse of the southern Sierra Nevada batholith, California: Geosphere, v. 8, no. 2, p. 314–341, https://doi.org/10.1130/GES00740.1.

Chapman, J.B., Ducea, M.N., DeCelles, P.G., and Profeta, L., 2015, Tracking changes in crustal thickness during orogenic evolution with Sr/Y: An example from the North America Cordillera: Geology, v. 43, no. 10, p. 919–922, https://doi.org/10.1130/G36996.1.

Chapman, J.B., Ducea, M.N., Kapp, P., Gehrels, G.E., and DeCelles, P.G., 2017, Spatial and temporal radiogenic isotopic trends of magmatism in Cordilleran orogens: Gondwana Research, v. 48, p. 189–204, https://doi.org/10.1016/j.gr.2017.04.019.

Chapman, J.B., Dafov, M.N., Gehrels, G., Ducea, M.N., Valley, J.W., and Ishida, A., 2018, Lithospheric architecture and tectonic evolution of the southwestern U.S. Cordillera: Constraints from zircon Hf and O isotopic data: Geological Society of America Bulletin, v. 130, no. 11–12, p. 2031–2046, https://doi.org/10.1130/B31937.1.

Chapman, A.D., Rautela, O., Shields, J., Ducea, M.N., and Saleeby, J., 2020a, Fate of the lower lithosphere during shallow-angle subduction: The Laramide example: GSA Today, v. 30, no. 1, p. 4–10, https://doi.org/10.1130/GSATG412A.1.

Chapman, J.B., Grieg, R., and Haxel, G.B., 2020b, Geochemical evidence for an orogenic plateau in the southern U.S. and northern Mexican Cordillera during the Laramide orogeny: Geology, v. 48, no. 2, p. 164–168, https://doi.org/10.1130/G47117.1.

Chen, J.H., and Tilton, G.R., 1991, Applications of lead and strontium isotopic relationships to the petrogenesis of granitoid rocks, central Sierra Nevada batholith, California: Geological Society of America Bulletin, v. 103, no. 4, p. 439–447, https://doi.org/10.1130/0016-7606(1991)103<0439:AOLASI>2.3.CO;2.

Coleman, D.S., and Glazner, A.F., 1997, The Sierra Crest magmatic event: Rapid formation of juvenile crust during the Late Cretaceous in California: International Geology Review, v. 39, no. 9, p. 768–787, https://doi.org/10.1080/00206819709465302.

Coney, P.J., and Reynolds, S.J., 1977, Cordilleran Benioff zones: Nature, v. 270, p. 403–406, https://doi.org/10.1038/270403a0.

Copeland, P., Currie, C.A., Lawton, T.F., and Murphy, M.A., 2017, Location, location, location: The variable life span of the Laramide orogeny: Geology, v. 45, no. 3, p. 223–226, https://doi.org/10.1130/G38810.1.

Davidson, J., Turner, S., Handley, H., Macpherson, C., and Dosseto, A., 2007, Amphibole "sponge" in arc crust?: Geology, v. 35, no. 9, p. 787–790, https://doi.org/10.1130/G23637A.1.

Davidson, J., Turner, S., and Plank, T., 2013, Dy/Dy*: Variations arising from mantle sources and petrogenic processes: Journal of Petrology, v. 54, no. 3, p. 525–537, https://doi.org/10.1093/petrology/egs076.

DePaolo, D., 1981, A neodymium and strontium isotopic study of the Mesozoic calc-alkaline granitic batholiths of the Sierra Nevada and Peninsular Ranges, California: Journal of Geophysical Research, v. 86, no. B11, p. 10470–10488, https://doi.org/10.1029/JB086iB11p10470.

Dickinson, W.R., Snyder, W.S., and Matthews, V., 1978, Plate tectonics of the Laramide orogeny, *in* Matthews, V., ed., Laramide Folding Associated with Basement Block Faulting in the Western United States: Geological Society of America Memoir 151, p. 355–366, https://doi.org/10.1130/MEM151-p355.

Dong, G., Mo, X.-x., Zhao, Z., Guo, T.-y., Wang, L.-l., and Chen, T., 2005, Geochronologic constraints on the magmatic underplating of the Gangdise belt in the India-Eurasia collision: Evidence of SHRIMP-II zircon U-Pb dating: Acta Geologica Sinica, v. 79, no. 6, p. 787–794, https://doi.org/10.1111/j.1755-6724.2005.tb00933.x.

Ducea, M.N., 2001, The California arc: Thick granitic batholiths, eclogitic residues, lithospheric-scale thrusting, and magmatic flare-ups: GSA Today, v. 11, no. 11, p. 4–10.

Ducea, M.N., and Saleeby, J.B., 1998, A case for delamination of the deep batholithic crust beneath the Sierra Nevada, California: International Geology Review, v. 40, no. 1, p. 78–93, https://doi.org/10.1080/00206819809465199.

Faulds, J.E., Feuerbach, D.L., Miller, C.F., and Smith, E.I., 2001, Cenozoic evolution of the northern Colorado River extensional corridor, southern Nevada and northwest Arizona, *in* Erskine, M.C., Faulds, J.F., Bartley, J.M., and Rowley, R.D., eds., The Geologic Transition, High Plateaus to Great Basin—A Symposium and Field Guide (The Mackin Volume): Salt Lake City, Utah, Utah Geological Association, p. 239–271.

Fleck, R.J., Wooden, J.L., Matti, J.C., Powell, R.E., and Miller, F.K., 1997, Geochronologic investigations in the Little San Bernardino Mountains, California: Geological Society of America Abstracts with Programs, v. 29, no. 5, p. 12–13.

Friesenhahn, B.P., 2018, The Transition from Sevier to Laramide Orogeny Captured in Upper-Plate, Syn-Magmatic Structures, Eastern Transverse Ranges, CA [Master's thesis]: Dallas, Texas, Southern Methodist University, 50 p.

Frost, B.R., Barnes, C.G., Collins, W.J., Arculus, R.J., Ellis, D.J., and Frost, C.D., 2001, A geochemical classification for granitic rocks: Journal of Petrology, v. 42, p. 2033–2048, https://doi.org/10.1093/petrology/42.11.2033.

Grove, M., Jacobson, C.E., Barth, A.P., and Vucic, A., 2003, Temporal and spatial trends of Late Cretaceous–early Tertiary underplating of Pelona and related schist beneath southern California and southwestern Arizona, *in* Johnson, S.E., Patterson, S.R., Fletcher, J.M., Girty, G.H., Kimbrough, D.L., and Martin-Barajas, A., eds., Tectonic Evolution of Northwestern Mexico and the Southwestern USA: Geological Society of America Special Paper 374, p. 381–406, https://doi.org/10.1130/0-8137-2374-4.381.

Haxel, G.B., and Dillon, J.T., 1978, The Pelona-Orocopia Schist and Vincent–Chocolate Mountain thrust system, southern California, *in* Howell, D.G., and McDougall, K.A., eds., Mesozoic Paleogeography of the Western United States: Los Angeles, California, Pacific Section, SEPM (Society for Sedimentary Geology), Pacific Coast Paleogeography Symposium 2, p. 453–469.

Heller, P.L., and Liu, L., 2016, Dynamic topography and vertical motion of the U.S. Rocky Mountain region prior to and during the Laramide orogeny: Geological Society of America Bulletin, v. 128, no. 5–6, p. 973–988, https://doi.org/10.1130/B31431.1.

Hildebrand, R.S., and Whalen, J.B., 2017, The Tectonic Setting and Origin of Cretaceous Batholiths within the North American Cordillera: The Case for Slab Failure Magmatism and its Significance for Crustal Growth: Geological Society of America Special Paper 532, 113 p., https://doi.org/10.1130/2017.2532.

Howard, K.A., 2002, Geologic Map of the Sheep Hole Mountains 30′ × 60′ Quadrangle, San Bernardino and Riverside Counties, California: U.S. Geological Survey Miscellaneous Field Studies Map 2344, scale 1:100,000, https://doi.org/10.3133/mf2344.

Howard, K.A., and John, B.E., 1987, Crustal extension along a rooted system of imbricate low-angle faults: Colorado River extensional corridor, California and Arizona, *in* Coward, M.P., Dewey, J.F., and Hancock, P.L., eds., Continental Extensional Tectonics: Geological Society [London] Special Publication 28, p. 299–311, https://doi.org/10.1144/GSL.SP.1987.028.01.19.

Howard, K.A., Wooden, J.L., Barnes, C.B., Premo, W.R., Snoke, A.W., and Lee, S.-Y., 2011, Episodic growth of a Late Cretaceous and Paleogene intrusive complex of pegmatitic leucogranite, Ruby Mountains core complex, Nevada, USA: Geosphere, v. 7, no. 5, p. 1220–1248, https://doi.org/10.1130/GES00668.1.

Howard, K.A., Bacheller, J., Fitzgibbon, T.T., Powell, R.E., and Allen, C.M., 2013, Geologic Map of the Valley Mountain 15′ Quadrangle, San Bernardino and Riverside Counties, California: U.S. Geological Survey Geologic Quadrangle Map GQ 1767, scale 1:62,500, https://doi.org/10.3133/gq1767.

Ianno, A.J., 2015, Studies of the Late Cretaceous Magmatic Crustal Column at Joshua Tree National Park, California [Ph.D. dissertation]: Los Angeles, California, University of Southern California, 298 p.

Jacobson, C.E., Barth, A.P., and Grove, M., 2000, Late Cretaceous protolith age and provenance of the Pelona and Orocopia Schists, southern California: Implications for evolution of the Cordilleran margin: Geology, v. 28, p. 219–222, https://doi.org/10.1130/0091-7613(2000)28<219:LCPAAP>2.0.CO;2.

Ji, W.-q., Wu, F.-y., Liu, C.-z., and Chund, S.-l., 2012, Early Eocene crustal thickening in southern Tibet: New age and geochemical constraints from the Gangdese batholith: Journal of Asian Earth Sciences, v. 53, p. 82–95, https://doi.org/10.1016/j.jseaes.2011.08.020.

Jones, C.H., Farmer, L.G., Sageman, B., and Zhong, S.-j., 2011, Hydrodynamic mechanism for the Laramide orogeny: Geosphere, v. 7, no. 1, p. 183–201, https://doi.org/10.1130/GES00575.1.

Kay, R.W., and Kay, S.M., 1993, Delamination and delamination magmatism: Tectonophysics, v. 219, p. 177–189, https://doi.org/10.1016/0040-1951(93)90295-U.

Kidder, S., and Ducea, M.N., 2006, High temperatures and inverted metamorphism in the schist of Sierra de Salinas, California: Earth and Planetary Science Letters, v. 241, no. 3–4, p. 422–437, https://doi.org/10.1016/j.epsl.2005.11.037.

Kidder, S., Ducea, M.N., Gehrels, G., Patchett, P.J., and Vervoort, J., 2003, Tectonic and magmatic development of the Salinian Coast Range belt, California: Tectonics, v. 22, no. 5, 1058, https://doi.org/10.1029/2002TC001409.

Kistler, R.W., and Ross, D.C., 1990, A Strontium Isotopic Study of Plutons and Associated Rocks of the Southern Sierra Nevada and Vicinity: U.S. Geological Survey Bulletin 1920, 20 p., https://doi.org/10.3133/b1920.

Lee, S.Y., Barnes, C.G., Snoke, A.W., Howard, K.A., Frost, C.D., 2003, Petrogenesis of Mesozoic, peraluminous granites in the Lamoille Canyon area, Ruby Mountains, Nevada, USA: Journal of Petrology, v. 44, no. 4, p. 713–732, https://doi.org/10.1093/petrology/44.4.713.

Lieu, W.K., and Stern, R.J., 2019, The robustness of Sr/Y and La/Yb as proxies for crust thickness in modern arcs: Geosphere, v. 15, no. 3, p. 621–641, https://doi.org/10.1130/GES01667.1.

Liu, L., Gurnis, M., Seton, M., Saleeby, J., Müller, R.D., and Jackson, J.M., 2010, The role of oceanic plateau subduction in the Laramide orogeny: Nature Geoscience, v. 3, p. 353–357, https://doi.org/10.1038/ngeo829.

Livaccari, R., 1991, Role of crustal thickening and extensional collapse in the tectonic evolution of the Sevier-Laramide orogeny, western United States: Geology, v. 19, no. 11, p. 1104–1107, https://doi.org/10.1130/0091-7613(1991)019<1104:ROCTAE>2.3.CO;2.

Macpherson, C.G., Dreher, S.T., and Thirlwall, M.F., 2006, Adakites without slab melting: High pressure differentiation of island arc magma, Mindanao, the Philippines: Earth and Planetary Science Letters, v. 243, no. 3–4, p. 581–593, https://doi.org/10.1016/j.epsl.2005.12.034.

Matti, J.C., and Morton, D.M., 1993, Paleogeographic evolution of the San Andreas fault in southern California: A reconstruction based on a new cross-fault correlation, *in* Powell, R.E., Weldon, R.J., and Matti, J.C., eds., The San Andreas Fault System: Displacement, Palinspastic Reconstruction and Geologic Evolution: Geological Society of America Memoir 178, p. 107–160, https://doi.org/10.1130/MEM178-p107.

Mayo, D.P., Anderson, J.L., and Wooden, J.L., 1998, Isotopic constraints on the petrogenesis of Jurassic plutons, southeastern California: International Geology Review, v. 40, p. 257–278, https://doi.org/10.1080/00206819809465209.

McCaffrey, K.J.W., Miller, C.F., Karlstrom, K.E., and Simpson, C., 1999, Synmagmatic deformation patterns in the Old Woman Mountains, SE California: Journal of Structural Geology, v. 21, no. 3, p. 335–349, https://doi.org/10.1016/S0191-8141(98)00107-2.

Miller, C.F., Hanchar, J.M., Wooden, J.L., Bennett, V.C., Harrison, T.M., Wark, D.A., and Foster, D.A., 1992, Source region of a granite batholith: Evidence from lower crustal xenoliths and inherited accessory minerals: Transactions of the Royal Society of Edinburgh–Earth Sciences, v. 83, p. 49–62, https://doi.org/10.1017/S0263593300007744.

Morton, D.M., and Miller, F.K., 2003, Preliminary Geologic Map of the San Bernardino 30 × 60 Quadrangle, California: U.S. Geological Survey Open-File Report 03-293, scale 1:100,000, http://pubs.usgs.gov/of/2003/of03-293/.

Nadin, E.S., and Saleeby, J., 2008, Disruption of regional primary structure of the Sierra Nevada batholith by the Kern Canyon fault system, California, *in* Wright, J.E., and Shervais, J.W., eds., Ophiolites, Arcs and Batholiths: A Tribute to Cliff Hopson: Geological Society of America Special Paper 438, p. 429–454, https://doi.org/10.1130/2008.2438(15).

Needy, S.K., Anderson, J.L., Wooden, J.L., Fleck, R.J., Barth, A.P., Paterson, S.R., Memeti, V., and Pignotta, G.S., 2009, Mesozoic magmatism in an upper- to middle-crustal section through the Cordilleran continental margin arc, Eastern Transverse Ranges, California, *in* Miller, R.B., and Snoke, A.W., eds., Crustal Cross Sections from the Western North American Cordillera and Elsewhere: Implications for Tectonic and Petrologic Processes: Geological Society of America Special Paper 456, p. 187–218, https://doi.org/10.1130/2009.2456(07).

Paterson, S.R., Okaya, D., Memeti, V., Economos, R.C., and Miller, R.B., 2011, Magma addition and flux calculations of incrementally constructed magma chambers in continental margin arcs: Combined field, geochronologic and thermal modeling studies: Geosphere, v. 7, p. 1439–1468, https://doi.org/10.1130/GES00696.1.

Paterson, S.R., Clausen, B., Memeti, V., and Schwartz, J.J., 2017, Arc magmatism, tectonism, and tempos in Mesozoic arc crustal sections of the Peninsular and Transverse Ranges, southern California, USA, *in* Kraatz, B., Lackey, J.S., and Fryxell, J.E., eds., Field Excursions in Southern California: Field Guides to the 2016 GSA Cordilleran Section Meeting: Geological Society of America Field Guide 45, p. 81–186, https://doi.org/10.1130/2017.0045(04).

Pearce, J.A., Stern, R.J., Bloomer, S.H., and Fryer, P., 2005, Geochemical mapping of the Mariana arc-basin system: Implications for the nature and distribution of subduction components: Geochemistry Geophysics Geosystems, v. 6, no. 7, Q07006, https://doi.org/10.1029/2004GC000895.

Pickett, D.A., and Saleeby, J.B., 1993, Thermobarometric constraints on the depth of exposure and conditions of plutonism and metamorphism at deep levels of the Sierra Nevada batholith, Tehachapi Mountains, California: Journal of Geophysical Research–Solid Earth, v. 98, no. B1, p. 609–629, https://doi.org/10.1029/92JB01889.

Powell, R.E., 1981, Geology of the Crystalline Basement Complex, Eastern Transverse Ranges, Southern California [Ph.D. dissertation]: Pasadena, California, California Institute of Technology, 441 p.

Powell, R.E., 1993, Balanced palinspastic reconstruction of pre–late Cenozoic paleogeology, southern California, *in* Powell, R.E., Weldon, R.J., and Matti, J.C., eds., The San Andreas Fault System: Displacement, Palinspastic Reconstruction, and Geologic Evolution: Geological Society of America Memoir 178, p. 1–106, https://doi.org/10.1130/MEM178-p1.

Powell, R.E., Matti, J.C., and Cossette, P.M., 2015, Geology of the Joshua Tree National Park Geodatabase: U.S. Geological Survey Open-File Report 2015-1175, GIS database, https://doi.org/10.3133/ofr20151175.

Pratson, E.L., Anderson, R.N., Dove, R.E., Mitchell, L., Silver, L.T., James, E.W., and Chappell, B.W., 1992, Geochemical logging in the Cajon Pass drill hole and its application to new oxide igneous rock classification scheme: Journal of Geophysical Research, v. 97, p. 5167–5180, https://doi.org/10.1029/91JB02643.

Profeta, L., Ducea, M.N., Chapman, J.B., Paterson, S.R., Henriquez-Gonzales, S.M., Kirsch, M., Petrescu, L., and DeCelles, P.G., 2015, Quantifying crustal thickness over time in magmatic arcs: Nature: Scientific Reports, v. 5, p. 17786, https://doi.org/10.1038/srep17786.

Saleeby, J., 2003, Segmentation of the Laramide slab—Evidence from the southern Sierra Nevada region: Geological Society of America Bulletin, v. 115, no. 6, p. 655–668, https://doi.org/10.1130/0016-7606(2003)115<0655:SOTLSF>2.0.CO;2.

Schott, R.C., and Johnson, C.M., 1998, Sedimentary record of the Late Cretaceous thrusting and collapse of the Salinia-Mojave magmatic arc: Geology, v. 26, no. 4, p. 327–330, https://doi.org/10.1130/0091-7613(1998)026<0327:SROTLC>2.3.CO;2.

Strickland, A., Wooden, J.L., Mattinson, C.G., Ushikubo, T., Miller, D., and Valley, J.W., 2013, Proterozoic evolution of the Mojave crustal province as preserved in the Ivanpah Mountains, southeastern California: Precambrian Research, v. 224, p. 222–241, https://doi.org/10.1016/j.precamres.2012.09.006.

Wells, M.L., and Hoisch, T.D., 2008, Delamination of mantle lithosphere as the cause of widespread Late Cretaceous extension and anatexis in the southwestern Cordilleran orogeny: Geological Society of America Bulletin, v. 120, p. 515–530, https://doi.org/10.1130/B26006.1.

Wells, M.L., Spell, T.L., and Grove, M., 2002, Late Cretaceous intrusion and extensional exhumation of the Cadiz Valley batholith, Iron Mountains, southeastern California: Geological Society of America Abstracts with Programs, v. 34, p. 178, https://gsa.confex.com/gsa/2002AM/webprogram/Paper40694.html.

Wells, M.L., Beyene, M.A., Spell, T.L., Kula, J.L., Miller, D.M., and Zanetti, K.A., 2005, The Pinto shear zone, a Laramide synconvergent extensional shear zone in the Mojave Desert region of the southwestern United States: Journal of Structural Geology, v. 27, p. 1697–1720, https://doi.org/10.1016/j.jsg.2005.03.005.

Wicklund, A.P., Andrews, R.S., Barber, G.A., and Johnson, R.J., 1990, Cajon Pass Scientific Drilling Project: Drilling overview, *in* Fuchs, K., Kozlovsky, Y.A., Krivtsov, A.I., and Zoback, M.D., eds., Super-Deep Continental Drilling and Deep Geophysical Sounding: New York, Springer-Verlag, p. 40–56, https://doi.org/10.1007/978-3-642-50143-2_5.

Wiegand, B.A., Barth, A.P., Wooden, J.L., Palmer, E.F., Brown, K.L., and Needy, S.L., 2007, Sr and Nd isotopic evolution in Late Cretaceous lower to upper crustal granitic rocks from the Transverse Ranges, southern California: Geological Society of America Abstracts with Programs, v. 39, no. 6, p. 407, https://gsa.confex.com/gsa/2007AM/webprogram/Paper127265.html.

Wooden, J.L., and Miller, D.M., 1990, Chronologic and isotopic framework for early Proterozoic crustal evolution in the eastern Mojave Desert region, SE California: Journal of Geophysical Research, v. 95, p. 20133–20146, https://doi.org/10.1029/JB095iB12p20133.

Wooden, J.L., Fleck, R.J., Matti, J.C., Powell, R.E., and Barth, A.P., 2001, Late Cretaceous intrusive migmatites of the Little San Bernardino Mountains, California: Geological Society of America Abstracts with Programs, v. 33, no. 3, p. 63, https://gsa.confex.com/gsa/2001CD/webprogram/Paper3952.html.

Wooden, J.L., Barth, A.P., Tosdal, R.M., Howard, K.A., Miller, D.M., 2018, Where did that granitoid come from? For the SW US, try checking its Pb isotopic composition: Geological Society of America Abstracts with Programs, v. 50, no. 6, paper no. 66–8, https://doi.org/10.1130/abs/2018AM-318244.

Wright, J.E., Howard, K.A., and Anderson, J.L., 1987, Isotopic systematics of zircons from Late Cretaceous intrusive rocks, southeastern California: Implications for a vertically stratified crustal column: Geological Society of America Abstracts with Programs, v. 19, p. 898.